MICROCOPY RESOLUTION TEST CHART

NATIONAL BUREAU OF STANDARDS-1963-A

MARTIN MARIETTA

Martin Marietta Laboratories

MML TR85-7(c)

MECHANICAL PROPERTIES OF ADHESIVELY
BONDED ALUMINUM STRUCTURES PROTECTED
WITH HYDRATION INHIBITORS

March 1985

DTIC
SELECTE
MAY 16 1985
A

Submitted to:

Department of the Navy
Office of Naval Research
800 North Quincy Street
Arlington, Virginia 22217

Submitted by:

MARTIN MARIETTA CORPORATION
Martin Marietta Laboratories
1450 South Rolling Road
Baltimore, Maryland 21227

85   105

REPORT DOCUMENTATION PAGE		READ INSTRUCTIONS BEFORE COMPLETING FORM
1. REPORT NUMBER	2. GOVT ACCESSION NO.	3. RECIPIENT'S CATALOG NUMBER
4. TITLE (and Subtitle) Mechanical Properties of Adhesively Bonded Aluminum Structures Protected with Hydration Inhibitors		5. TYPE OF REPORT & PERIOD COVERED FINAL REPORT 5/1/82 – 1/31/85
		6. PERFORMING ORG. REPORT NUMBER MML TR85-7c
7. AUTHOR(s) G. D. Davis, J. S. Ahearn and J. D. Venables		8. CONTRACT OR GRANT NUMBER(s) N00014-80-C-0718
9. PERFORMING ORGANIZATION NAME AND ADDRESS Martin Marietta Corporation Martin Marietta Laboratories 1450 S. Rolling Road Baltimore, MD 21227-3898		10. PROGRAM ELEMENT. PROJECT, TASK AREA & WORK UNIT NUMBERS
11. CONTROLLING OFFICE NAME AND ADDRESS Department of the Navy Office of Naval Research Arlington, VA 22217		12. REPORT DATE March, 1985
		13. NUMBER OF PAGES 87
14. MONITORING AGENCY NAME & ADDRESS(if different from Controlling Office)		15. SECURITY CLASS. (of this report) UNCLASSIFIED
		15a. DECLASSIFICATION/DOWNGRADING SCHEDULE

16. DISTRIBUTION STATEMENT (of this Report)

Unlimited distribution

17. DISTRIBUTION STATEMENT (of the abstract entered in Block 20, if different from Report)

18. SUPPLEMENTARY NOTES

19. KEY WORDS (Continue on reverse side if necessary and identify by block number)

Adhesive bonding, organic inhibitors, mechanical testing, aluminum.

20. ABSTRACT (Continue on reverse side if necessary and identify by block number)

The use of hydration inhibitors to improve the durability of adhesively bonded aluminum structures was investigated. Pretreatment of Forest Products Laboratory (FPL) adherends in a solution of an inhibitor, such as nitrilotris methylene phosphonic acid (NTMP), increases bond durability dramatically, so that, in some cases, hydration of the adherend is no longer the limiting step in crack propagation. Pretreatment of phosphoric-acid-anodized (PAA) adherends further improves durability so that the transition to failure in the adhesive
(continued)

DD FORM 1473 1 JAN 73   EDITION OF 1 NOV 65 IS OBSOLETE

occurs at a shorter crack length. The initial strength for bonds using epoxy adhesives is not changed by such pretreatments. Adsorption of NTMP onto FPL surfaces displaces the water initially present by the formation of P-O-Al bonds. Saturation coverage is approximately one monolayer. Adsorption of NTMP onto PAA surfaces, which have little initial water, results in the occupation of residual active sites. Hydration of an inhibited FPL surface proceeds in three steps: i) reversible physi-sorption of water, ii) slow dissolution of the inhibitor-aluminum complex followed by rapid hydration of the freshly exposed amorphous aluminum oxide to boehmite, and iii) further hydration of the boehmite to bayerite. Finally, several criteria important for inhibitors designed to improve bond durability were identified: i) displacement of water and occupation of all active sites on the Al_2O_3 surface, ii) formation of strong inhibitor surface bonds, iii) insolubility of the resulting inhibitor-aluminum complex in aqueous solutions, iv) compatibility with the adhesive or primer, and v) coupling of the inhibitor to the adhesive.

MML TR 85-7c

MECHANICAL PROPERTIES OF ADHESIVELY BONDED ALUMINUM
STRUCTURES PROTECTED WITH HYDRATION INHIBITORS

Final Report on

ONR Contract N00014-80-C-0718

March 1985

Prepared for:

Department of the Navy
Office of Naval Research
800 North Quincy Street
Arlington, Virginia 22217

Prepared by:

G.D. Davis, J.S. Ahearn, and J.D. Venables
MARTIN MARIETTA CORPORATION
Martin Marietta Laboratories
1450 South Rolling Road
Baltimore, Maryland 21227

G.D. Davis
Principal Investigator

TABLE OF CONTENTS

ii

LIST OF FIGURES

v

LIST OF TABLES

ABSTRACT

The investigation of the use of hydration inhibitors to improve the durability of adhesively bonded aluminum structures, performed under ONR contract N00014-80-C-0718, is reviewed and summarized. Pretreatment of Forest Products Laboratory (FPL) adherends in a solution of an inhibitor, such as nitrilotris methylene phosphonic acid (NTMP), increases bond durability dramatically, so that, in some cases, hydration of the adherend is no longer the limiting step in crack propagation. Pretreatment of phosphoric-acid-anodized (PAA) adherends further improves durability so that the transition to failure in the adhesive occurs at a shorter crack length. The initial strength for bonds using epoxy adhesives is not changed by such pretreatments. Adsorption of NTMP onto FPL surfaces displaces the water initially present by the formation of P-O-Al bonds. Saturation coverage is approximately one monolayer. Adsorption of NTMP onto PAA surfaces, which have little initial water, results in the occupation of residual active sites. Hydration of an inhibited FPL surface proceeds in three steps: i) reversible physisorption of water, ii) slow dissolution of the inhibitor-aluminum complex followed by rapid hydration of the freshly exposed amorphous aluminum oxide to boehmite, and iii) further hydration of the boehmite to bayerite. Finally, several criteria important for inhibitors designed to improve bond durability were identified: i) displacement of water and occupation of all active sites on the Al_2O_3 surface, ii) formation of strong inhibitor surface bonds, iii) insolubility of the resulting inhibitor-aluminum complex in aqueous solutions, iv) compatibility with the adhesive or primer, and 5) coupling of the inhibitor to the adhesive.

I. INTRODUCTION

Adhesively-bonded aluminum is commonly used in aerospace structures and other applications that require light-weight, but strong, material. The design of any joint helps to determine its performance. However, a properly designed structure will live up to its potential only if stresses are transferred between the adherends through the adhesive. If this is not the case, interfacial failure will occur prior to reaching the theoretical performance limit.

The performance of an adhesively bonded structure is judged both by the initial bond strength and the long-term durability of the bond. The high initial interfacial strength provided by commercial aerospace bonding processes[1,2] is a consequence of the microscopically rough aluminum oxide formed during the etching or anodization treatment. When polymeric adhesive is added, it penetrates the oxide pores and surrounds the oxide whiskers to form a physical interlocking that ensures a much stronger bond than that possible with the purely chemical forces of a smooth oxide surface.[3-5]

The oxide morphology also partially governs long-term bond durability in moist environments in that the mechanical interlocking of an adhesive and a rough aluminum oxide can maintain high bond strength even if the chemical interaction between the oxide and polymer is diminished. In this case, a crack propagates only if interlocking is destroyed or failure occurs cohesively in the adhesive. In early work at Martin Marietta Laboratories, we showed that crack propagation during exposure to high humidity occurred as the aluminum oxide hydrated to the oxyhydroxide, boehmite, allowing failure either at the boehmite-metal or boehmite-adhesive interface prior to a cohesive failure in the adhesive, which is the ultimate performance limit of any given adhesive bond.[6,7]

Under contract N00014-80-C-0718,[4,7-18] we have extended this work to determine 1) the behavior of the surface chemistry of Forest Products

-1-

Laboratory (FPL)-etched adherends and, to a lesser extent, phosphoric-acid-anodized (PAA) adherends during adsorption of various hydration inhibitors, such as nitrilotris methylene phosphonic acid [NTMP];[19] 2) the procedure by which the treated FPL surfaces eventually hydrate; 3) the mechanism of crack propagation in a moist environment for treated and untreated FPL- and PAA-prepared structures; 4) the relative effectiveness of several related inhibitors in improving durability of FPL bonds, and 5) the effect of these inhibitors on the initial bond strength. Based on our results, we have identified five criteria or properties for hydration inhibitors designed to enhance bond durability.

In the course of this investigation we have applied a varied and multidisciplinary approach ranging from sophisticated surface analysis to fracture mechanics. The synthesis of all these techniques has allowed the enhanced understanding of the processes involved.

II. EXPERIMENTAL PROCEDURE

A. SURFACE PREPARATION

Test coupons and panels of bare 2024 Al were degreased by 15-min immersion in an agitated solution of Turco 4215* (44 g/l) at 65°C and then rinsed in distilled, deionized water. Degreasing was followed by a standard FPL treatment,[1] consisting of a 15-min immersion in an agitated aqueous solution of sodium dichromate dihydrate (60 g/l) and sulfuric acid (17% v/v) held at 65°C, after which samples were rinsed in distilled, deionized water and air dried. Some FPL-treated panels were then treated using the PAA process.[2] These panels were anodized in a 10%(w/w) phosphoric acid solution at a potential of 10 V for 20 min, rinsed in distilled, deionized water, and air dried.

The coupons were immersed for 30 min in a dilute aqueous solution of the inhibitor held at room temperature or, for a few selected cases, at 80°C. Solution concentrations ranged from 0.1 to 500 ppm for the adsorption experiments and from 10 to 300 ppm for the hydration studies and mechanical tests. The samples were then thoroughly rinsed in distilled, deionized water, forced-air dried, and stored in a dessicator until analysis.

Most samples used in the hydration experiments were suspended vertically in a humidity chamber and exposed to air saturated with water vapor at 50°C. The samples were removed at different intervals, dried with forced air, and also stored in a dessicator prior to surface analysis using X-ray photoelectron spectroscopy (XPS).

Incubation time measurements were made by direct visual observation and ellipsometry. For both methods, deionized, distilled water was boiled for 5

---

* An alkaline cleaning agent manufactured by Turco Products, Los Angeles, CA

min to lower the dissolved O_2 concentration and then cooled to 80°C. For visual observations, the sample was immersed in the water and the time after immersion when the color of the surface changed and gas bubbles appeared was noted. The color change was a direct indication that the Al oxide had hydrated [as confirmed by examining the sample by ultra-high resolution scanning electron microscopy (X-SEM)].

Ellipsometry measurements were made using a null balance technique where the polarizer and analyzer are rotated to extinguish the light. The point of extinction represents a null point, which is specific for the thickness and optical constants of the film. Any subsequent change in the film's nature changes the null point. When the Al oxide starts to hydrate, the null point settings for the polarizer and analyzer change. Thus, if the polarizer and analyzer are left unchanged during a measurement, an increase in the light intensity, as recorded by a photomultiplier, signals the onset of hydration.

B. SURFACE ANALYSIS

The XPS measurements were made on a Physical Electronics Model 548 spectrometer, which consists of a double-pass cylindrical mirror analyzer (CMA) with pre-retarding grids and a coaxial electron gun, a Mg anode X-ray source, a rastering 5-keV sputter ion gun, a sample introduction device, and a gas-handling system used to backfill the chamber to 5×10^{-5} Torr Ar. Operating pressure was in the low 10^{-9} Torr range. The XPS measurements were sometimes supplemented by Auger electron spectroscopy (AES) and ion sputtering to obtain an elemental distribution with depth.

Atomic concentrations were determined from either low-resolution (200-eV pass energy) survey spectra or, for higher accuracy, high-resolution (50-eV pass energy) spectra o⌐ the O1s, Al2p, and P2p peaks.[20] These results were interpreted with the use of surface behavior diagrams (SBD's),[20-21] a recently developed method for analyzing quantitative surface-sensitive

results. Although resembling ternary or quaternary phase diagrams in that they represent the surface composition as the sum of the compositions of three or four basis compounds, SBD's differ in that they display surface compositional, rather than bulk structural, data. In addition, the equilibrium condition is relaxed for SBD's, so that the surface can be described during such non-equilibrium processes such as hydration. To this end, the SBD's graphically display the changes in surface composition as a function of reaction time, solution concentration, anodization voltage, depth in the sample, or other parameters of interest. The measured changes can then be compared with those predicted by various models.

In this study, the atomic concentrations of O, Al, and P were usually converted to molar concentrations of Al_2O_3, inhibitor, and H_2O. This was done on the assumption that all the P was assigned to the inhibitor, the Al was assigned to Al_2O_3, and enough O was used to satisfy the inhibitor and Al_2O_3 stoichiometric requirements. Any excess O was assumed to be bonded to H as H_2O. For example, AlOOH has a composition equivalent to $Al_2O_3 + H_2O$ even though it is not a two-phase mixture of these compounds. The molar concentrations were then plotted on the appropriate SBD. In certain cases, the atomic concentrations were also directly plotted onto an Al-P-O SBD.

C. MECHANICAL TESTING

Following surface preparation, wedge-test adherends (150 mm x 150 mm x 3 mm) were bonded together using American Cyanamid FM 123-2 adhesive cured at 120°C for 1 hour (Table I). The adhesive consists of a Dacron mat impregnated with an epoxy-based resin. These bonded panels were cut into five 25-mm x 15-mm test pieces and wedges (3 mm thick) were inserted between the two adherends to provide a stress at the bondline. After an equilibration period of 1 hour at ambient conditions, the test samples were placed in a humidity chamber held at 60°C and 98% relative humidity. Periodically, the test pieces were removed from the chamber and examined under an optical microscope to

locate and mark the position of the crack front. When the test was complete, usually after 150 to 160 hours, calipers were used to measure the positions of the marks, which denoted crack length as a function of time.

The wedge test conditions (a water-wicking adhesive, high temperature, and no corrosion-inhibiting primer) were used to accelerate the testing procedure. In all cases (except one described below), once the test pieces were inserted into the humidity chamber, the crack appeared to propagate adhesively. This is an important requirement of the test since the relative effectiveness of different inhibitors can only be determined if the failure is adhesive.

Wedge-test specimens are the adhesive-joint analog of the wedge-force loaded double-cantilever beam (DCB) specimen used in the testing of homogeneous materials. Combining simple beam theory and linear elastic fracture mechanics,[22] the energy released per unit area is given by:

$$G = \frac{3h^3Ew^2}{16a^4} \tag{1}$$

where E = Young's modulus of the adherends, h = thickness of the adherends, w = wedge thickness, and a = crack length, measured from the point of load application. This equation can be modified to take into account such factors as ductile strain in the adhesive which would allow rotation of the adherends ahead of the crack tip.[23] Because the test was used in a comparative way only and the same adhesive was always employed, such corrections were not used in this analysis.

The crack-length data generated by the wedge test was used to calculate G in the aforementioned equation. The average crack velocity, was also determined from the information on crack length as a function of time.

On completion of the wedge test, the matching failure surfaces were separated along the opposite direction. Selected samples were then examined

using XPS, Auger depth profiling, or X-SEM in a JEOL-100CX STEM. Charging of the surface by the electron beam was suppressed without altering the very fine surface morphology on the specimen surface by secondary ion deposition of an extremely thin Pt coating.

Panels for T-peel tests (150 mm x 300 mm x 0.8 mm) were bonded together using the adhesives and cures listed in Table I. The panels were then cut into 25-mm strips and pulled using an Instron Model 1128 Tensile Testing machine with a cross-head speed of 3.3 mm/s.

Double lap-shear specimens, with a bond area of 25 mm x 12.5 mm on each side of the center panel (modified ASTM D 3528 Type A), were constructed using either FM 123-2 or Cybond 1102 as described in Table I. Adhesive thickness for the Cybond 1102 was controlled by a loop of 8-mil wire. The structures were then pulled using an Instron Model TTCL tensile testing machine with a cross-head speed of 0.0022 mm/s. In one experiment, double lap-shear specimens were hung for 7 days in the humidity chamber under the conditions described above for 7 days. They were then removed, wrapped with polyethylene to maintain the moist environment, and pulled using the Model TTCL instrument.

D. INHIBITOR SELECTION

Each of the compounds shown in Figs. 1 and 2 was selected to investigate various aspects of the inhibition process. NTMP served as our standard; most of our effort involved this compound. Adsorption of phosphoric acid [PA] onto FPL surfaces provided a chemical analog to the PAA surface without its more complex morphology.[3] Methylene phosphonic acid [MP] and amino methylene phosphonic acid [AMP] represented portions of the NTMP molecule, e.g., one "leg" and the central N with one "leg". Next, the two (butyl) nitrilobis methylene phosphonic acid isomers, [(n Bu)NBMP and (t Bu)NBMP], each possess two phosphonic acid "legs"; the first inhibitor exposes an extended hydrophobic hydrocarbon chain for possible micro-mechanical interlocking with the adhesive while the second exposes a compact

Table I

Mechanical Testing Parameters

Adhesive	Chemistry	Cure	Test
FM 123-2	Nitrile Epoxy	120°C, 280 kPa-1 hr	Wedge Double-Lap-Shear
FM 123-5	Nitrile Epoxy	110°C, 280 kPa-45 min	T-peel
FM 238/BR 238	Nitrile Phenolic	170°C, 280 kPa-1 hr	T-peel
FM 1000-EP15	Polyamide Epoxy	170°C, 280 kPa-1 hr	T-peel
FM 53	Epoxy	120°C, 280 kPa-1 hr	T-peel
Cybond 1102	Polyamide Epoxy	RT[a], 520 kPa-7 days	Double-Lap-Shear

[a] RT = room temperature
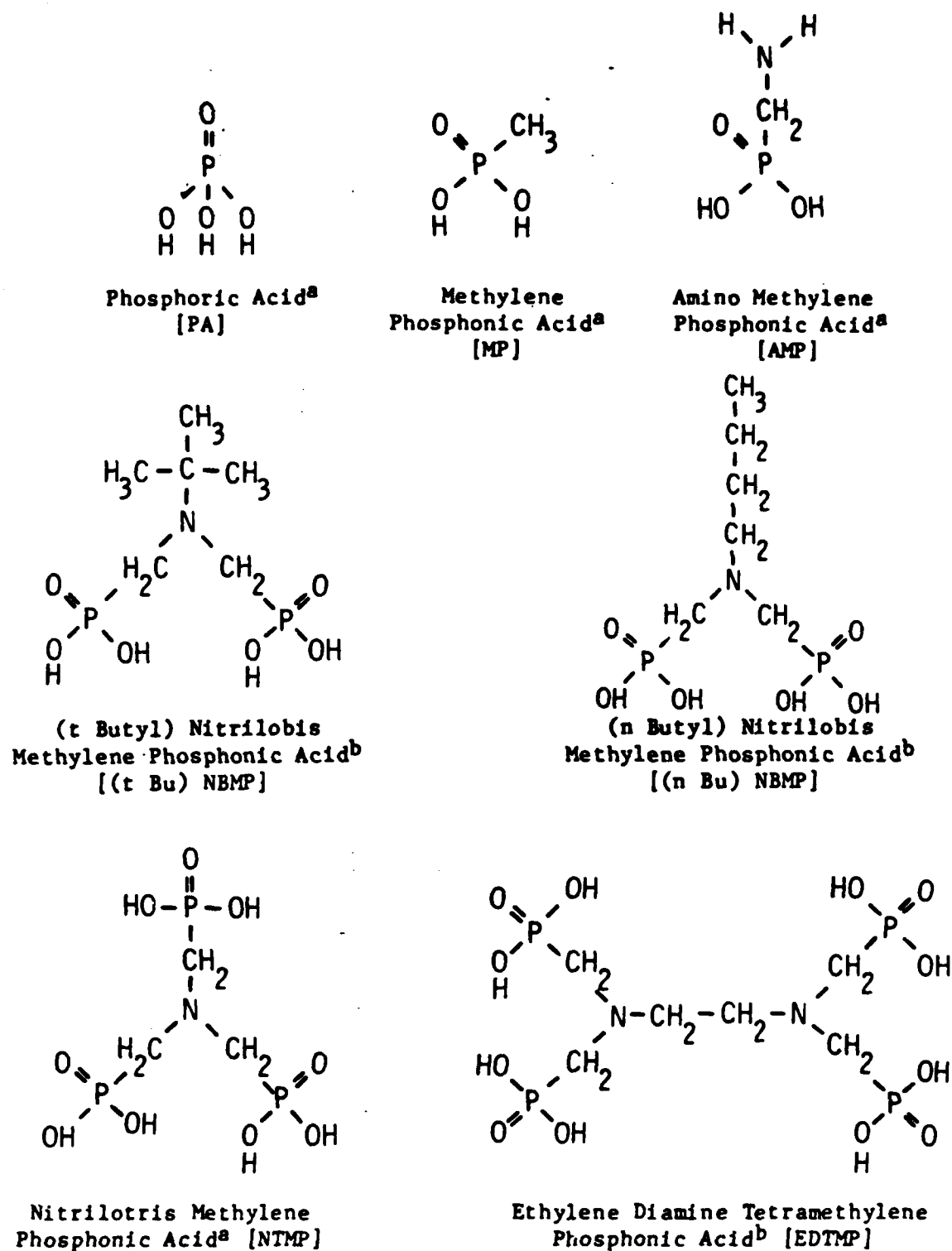
Figure 1. Inhibitors initially tested in this program: a) denotes compounds commercially available, and b) denotes compounds synthesized here. [17]

2Φ
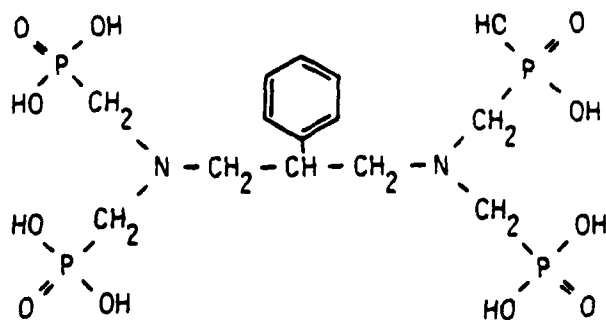
2-phenyl 1,3-di (nitrilobismethylene phosphonic acid) propane

2pA
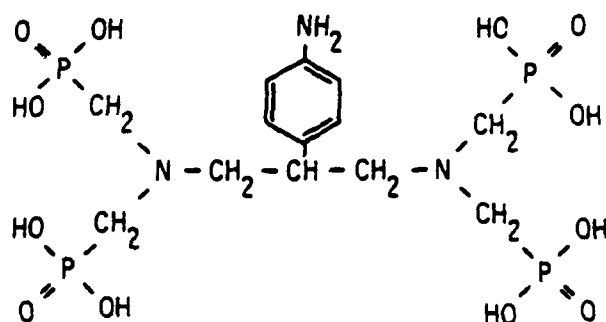
2-p-anilino 1,3-di (nitrilobismethylene phosphonic acid) propane

(nBu)ANBMP
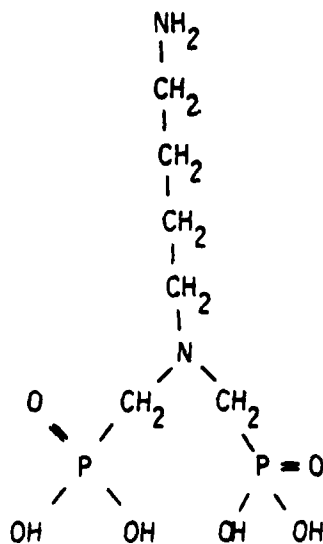
(n-butyl) aminonitrilobis methylene phosphonic acid

Figure 2. Additional inhibitors synthesized and tested.[10]

hydrocarbon cluster which should be chemically and mechanically inert. The (n Bu)NBMP was also modified by placing a chemically reactive group at the end of the hydrocarbon chain: (n-butyl) aminonitrilobis methylene phosphonic acid [(n Bu)ANBMP]. The remaining inhibitors, ethylene diamine tetramethylene phosphonic acid [EDTMP], 2-phenyl 1,3 di(nitrilobis methylene phosphonic acid) propane [2ø], and 2-p-anilino 1,3 di(nitrilobis methylene phosphonic acid) propane [2pA], increase the potential bonding sites to the aluminum oxide surface (POH groups, 2 per "leg") to eight. In addition, 2pA contains an amino group suitable for reacting with the epoxy adhesive.

III. RESULTS

A. FOREST PRODUCTS LABORATORY SURFACES

1.   Surface Chemistry

    a. Inhibitor Adsorption

    The adsorption of NTMP on the FPL surface has been studied as a
function of solution concentration and immersion time. A typical XPS spectrum
is shown in Fig. 3. The Al and most of the O are derived from the aluminum
oxide surface; the Cu signal comes from a Cu build-up in the metal just below
the oxide[24] and from Cu-rich inclusions near the surface.[4] Adsorbed NTMP
is evidenced by P, N, and some of the O and C. The remainder of the C arises
from adventitous hydrocarbon contamination.

    The dependence of the surface coverage and composition on solution
concentration is shown in the adsorption isotherm (Fig. 4) and in the Al_2O_3-
NTMP-H_2O SBD (Fig. 5). In the SBD, the solution concentration increases from
left to right. The approximately horizontal portion of the curve corresponds
to the saturation coverage of P/Al $\simeq$ 0.15 (~1 molecular layer) observed in
Fig. 4 above ~10 ppm. [The saturation coverage is rapidly obtained on FPL
surfaces -- no change in the surface composition was seen following immersion
periods of 5 s to 30 min.[17]] However, at elevated temperatures (Table II)
multiple inhibitor layers are formed.

    The adsorption process at room temperature can be described as the
displacement by NTMP of water or hydroxyl groups initially bound to the
aluminum oxide surface (illustrated schematically in Fig. 6) and the formation
of Al-O-P bonds, which is indicated by Fourier transform infrared (FTIR)
spectroscopy measurements on NTMP and an Al-NTMP complex.[17]

    Similar adsorption studies determining the saturation coverage (Table
II) or the effect of solution concentration were done for some of the other
inhibitors, including AMP. The adsorption of all phosphonates tested (e.g.,
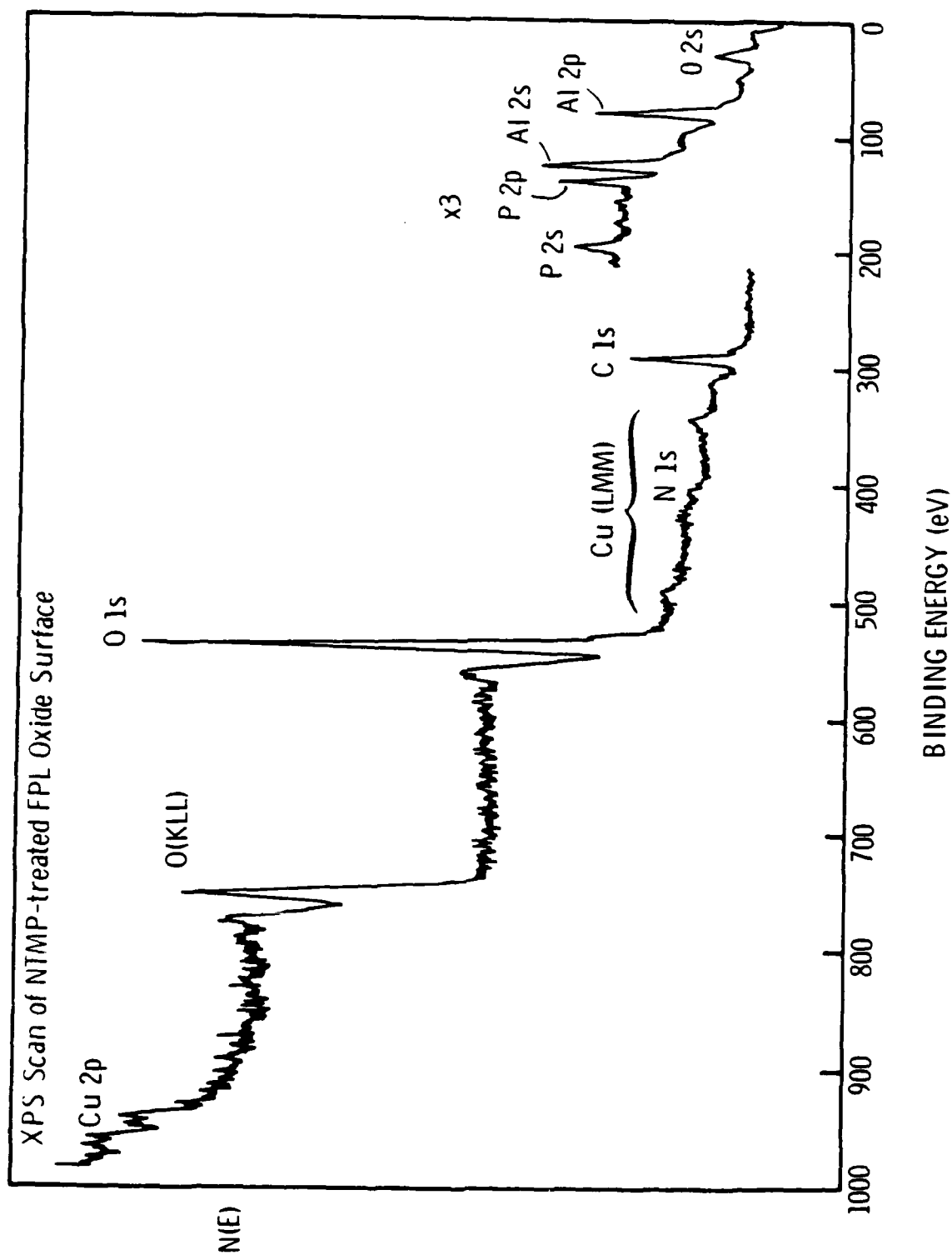
Figure 3. XPS spectrum of NTMP-treated FPL oxide surface.[11]
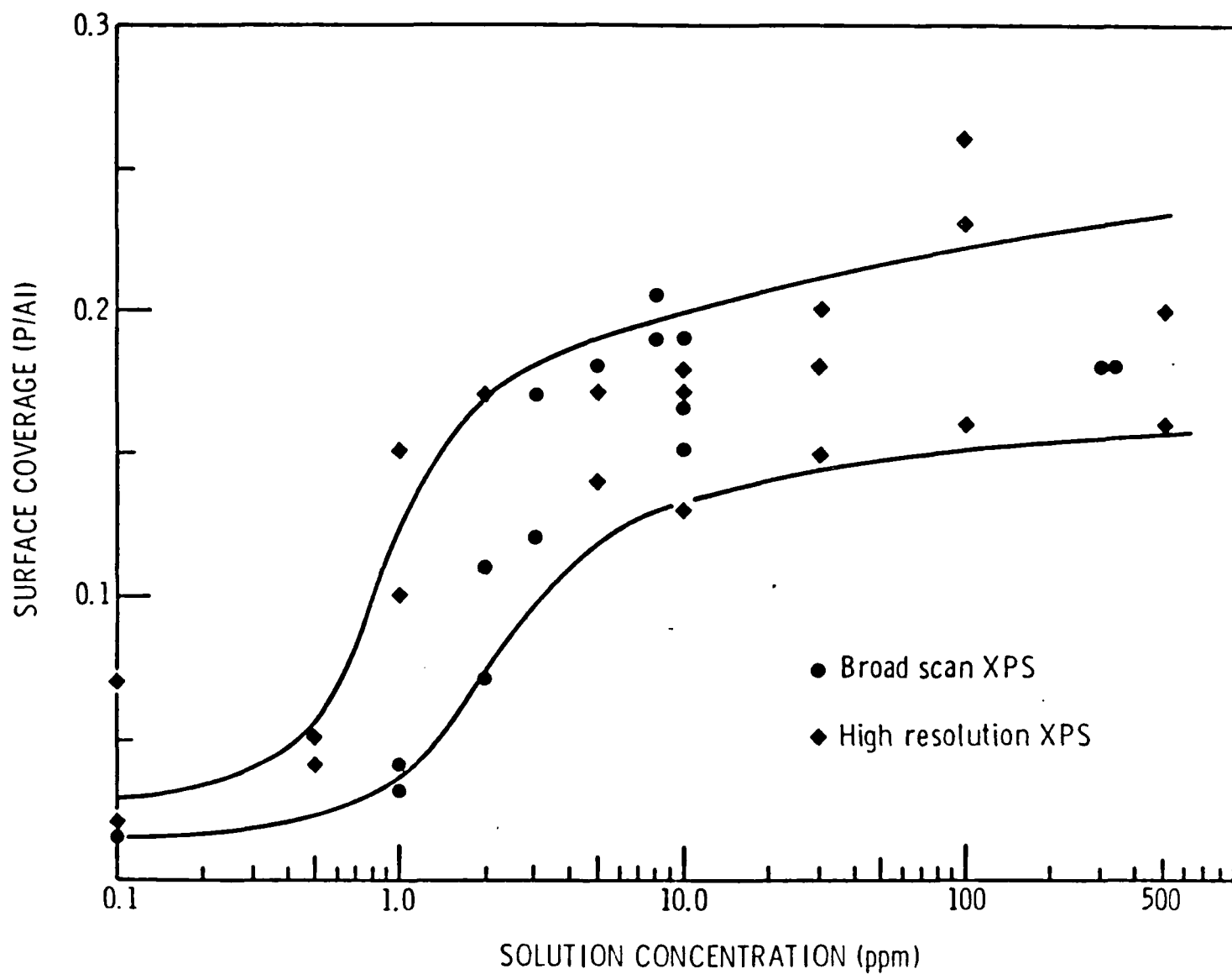
Figure 4. Surface coverage of NTMP-treated FPL oxide surface (P/Al) as a function of NTMP solution concentration.[14]
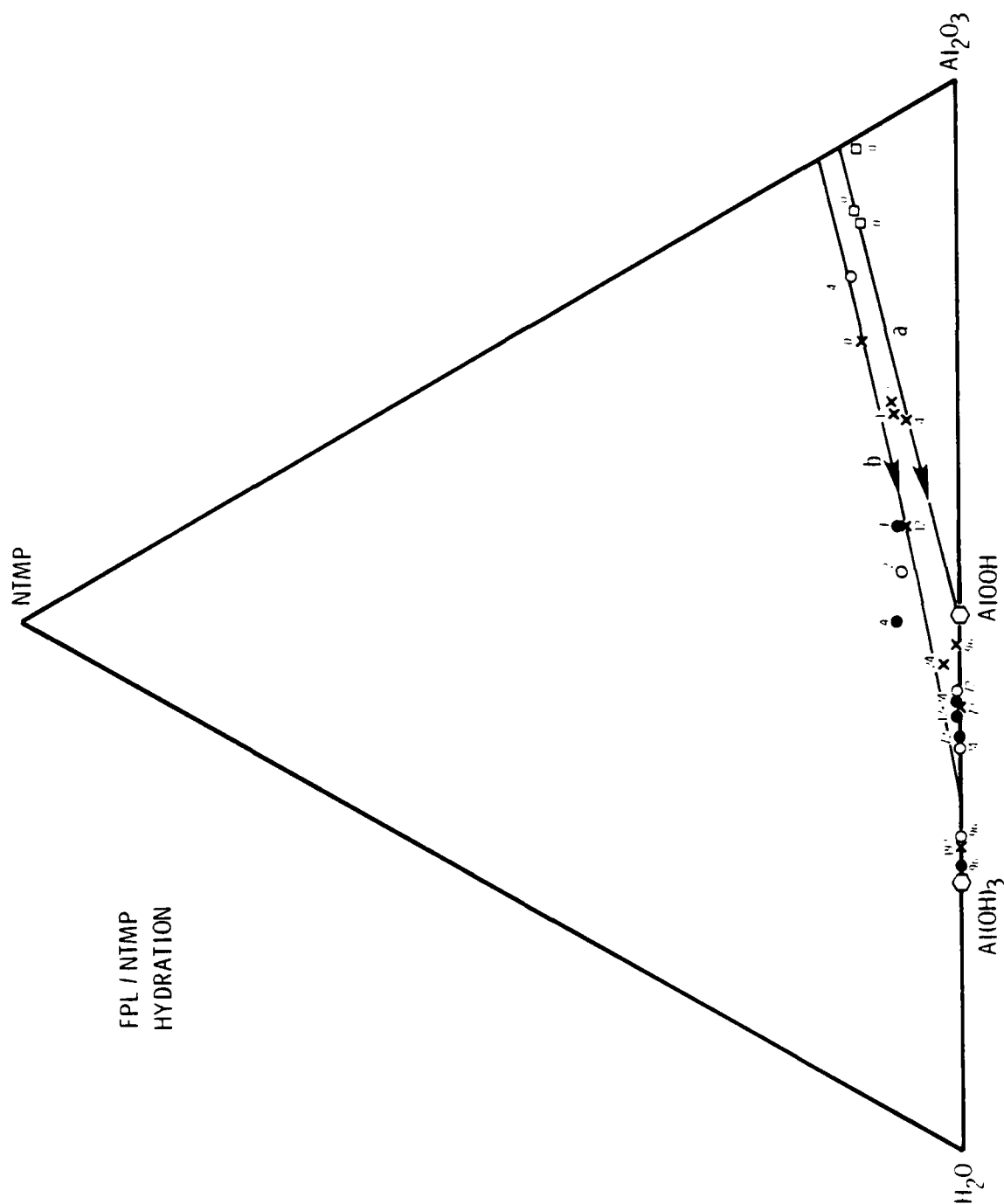
Figure 5. Al_2O_3–NTMP–H_2O SBD showing a) FPL-etched surface compositions after 30 min. immersion in aqueous solutions of NTMP at concentrations ranging from 0.1 to 500 ppm, solution concentration increases from left to right; and b) the path representing no displacement of water. (15)

Table II

Saturation Inhibitor Surface Coverage for
FPL-etched Adherends

Inhibitor and Treatment Temperature	Surface Coverage (XPS P/Al ratio)
NTMP, RT	0.15-0.2
NTMP, 80°C	0.4
PA, RT	0.1
AMP, RT	0.05-0.1
(n Bu)NBMP, RT	0.1-0.2
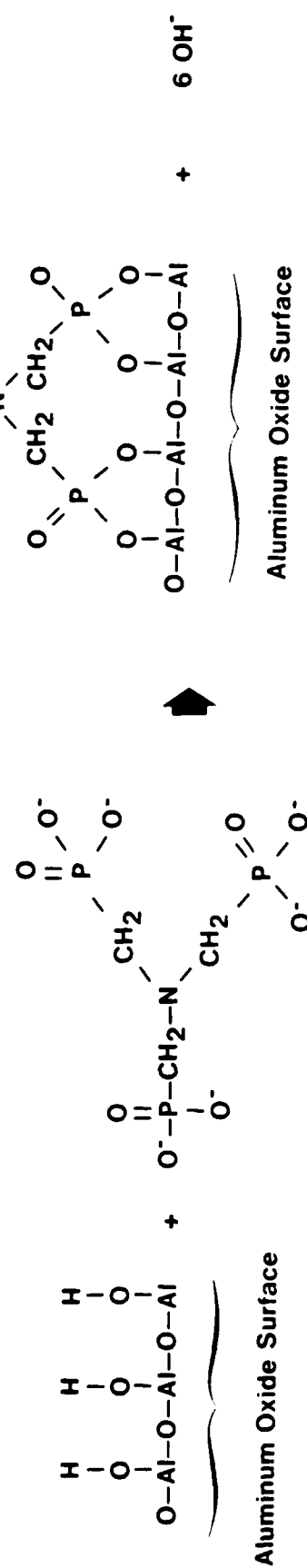
MODEL FOR ADSORPTION OF NTMP ON Al₂O₃

Figure 6. Schematic representation of NTMP adsorption onto FPL surfaces.[4]

Fig. 7) is qualitatively similar to that of NTMP on FPL, i.e., a displacement reaction of the inhibitor in exchange for adsorbed water. Subtle differences between the NTMP and AMP adsorption behavior, which are reflected in the different evolutionary paths in the A-P-O elemental SBD shown in Fig. 8, will be discussed later.

b. Hydration

The incubation time until hydration and/or the surface chemistry during hydration was measured for untreated FPL surfaces and surfaces treated with an inhibitor. The incubation time for conversion of oxide to hydroxide for FPL-etched coupons was approximately 2 min (Table III). Treatment of the FPL surface with any of the inhibitors tested (NTMP, AMP, or PA) increased this time considerably. Most of the incubation-time work was done with NTMP and in this case some coupons with saturation coverage hydrated in 12 min, whereas others did not hydrate at all after 5 days of immersion in water at 80°C.

One cause of the considerable scatter observed in the incubation-time measurements of the inhibitor-treated coupons is believed to be inclusions in the 2024 Al samples which can act as nucleation sites for hydration because of local galvanic currents and/or a discontinuous aluminum oxide film.[4] In any case, while the measurements do demonstrate increased resistance to hydration, they cannot be used to compare the effectiveness of different inhibitors. [Wedge test results discussed later (p. 26) do allow such a comparison].

The mechanism of hydration of NTMP-treated FPL surfaces was also investigated, using XPS and SBD's. As shown in Fig. 9, the hydration path proceeds from an NTMP-covered Al_2O_3 surface to a boehmite [AlOOH] surface (line "a") and then to one of bayerite [$Al(OH)_3$]. Variation in these data is caused by physisorbed water,[17,20] represented by line "b", which was calculated by the addition of approximately one monolayer of water to the surface compositions along line a. Surfaces with compositions along line b lost this physisorbed water after several days exposure to ultrahigh vacuum
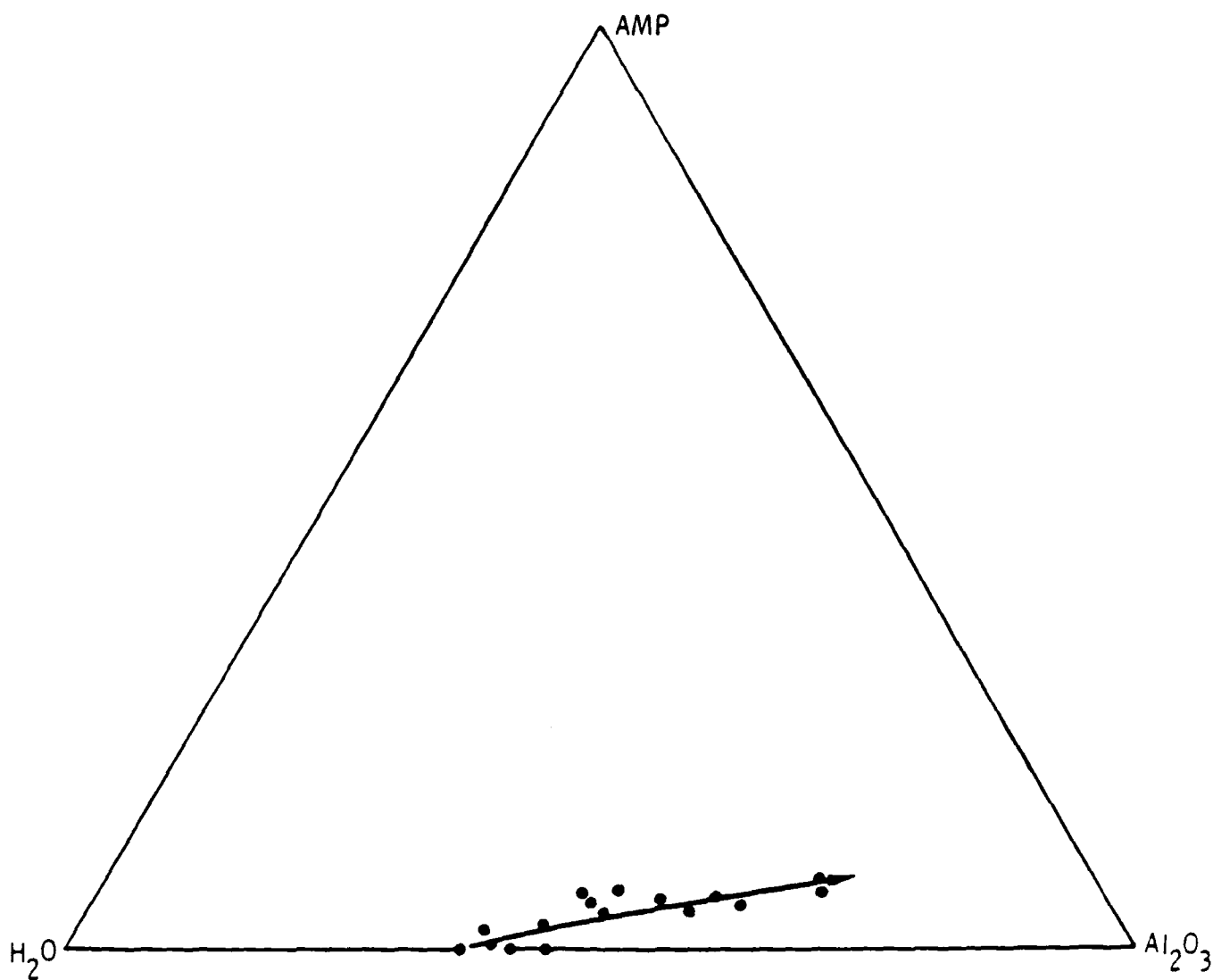
Figure 7. Al_2O_3-AMP-H_2O SBD of FPL-etched surface compositions after immersion in solutions of AMP at concentrations of 1 to 300 ppm.[17]
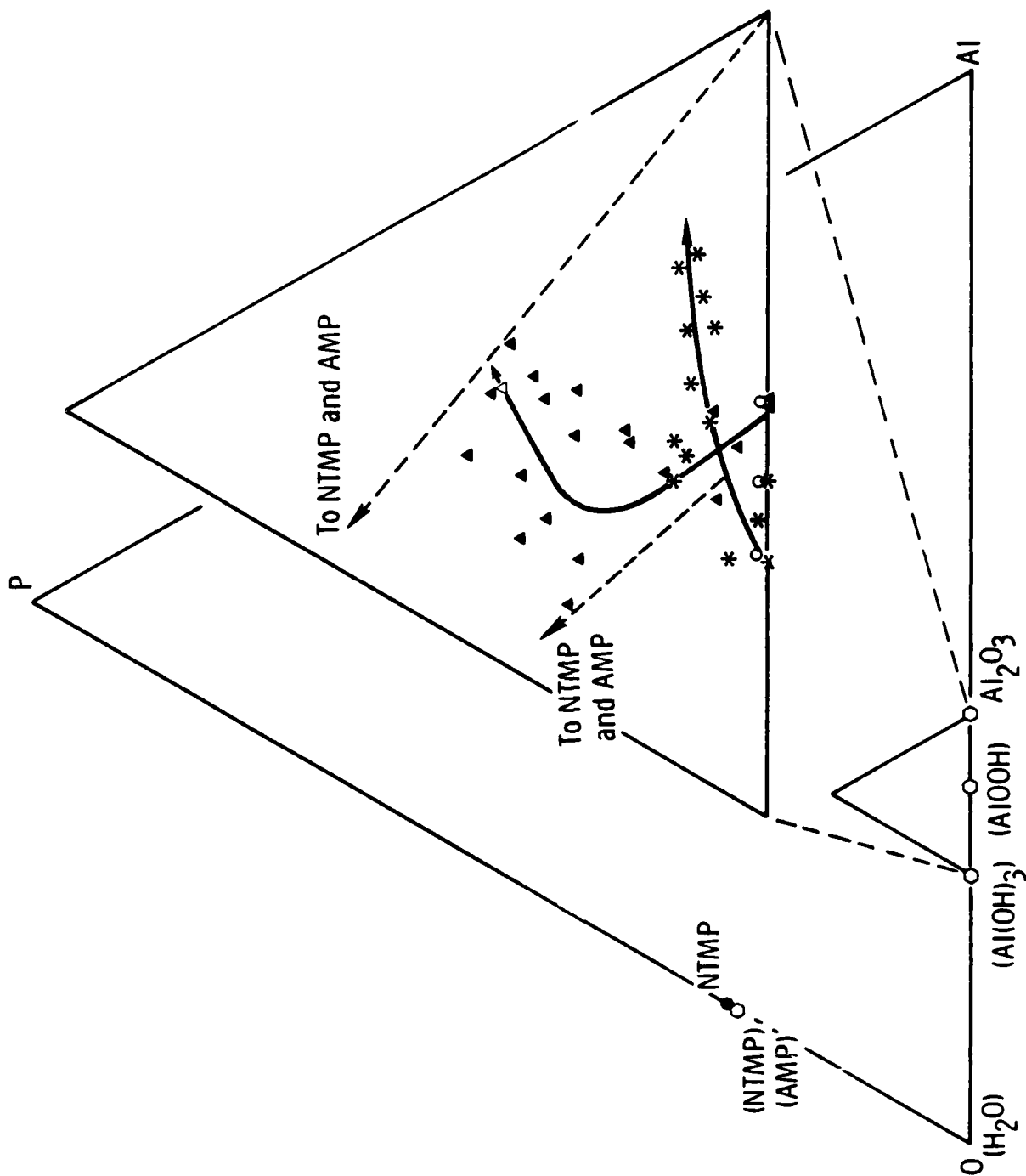
Figure 8. Al-P-O SBD of FPL-etched surface compositions after immersion in solutions of NTMP (triangles) or AMP (stars) at various concentrations. Open hexagons are calculated compositions. Compositions denoted by "0" represent surfaces not immersed in NTMP solutions.[1]

- 20 -

Table III

Incubation Time for FPL-Etched
Surfaces Treated in Different Hydration Inhibitors

Sample Description	Incubation Time (min)
FPL, no inhibitor treatment	1.5-2.0[a]
FPL + 10 ppm NTMP	360[a]
FPL + 100 ppm NTMP	indefinite[b]
FPL + 100 ppm NTMP	12[a]
FPL + 100 ppm AMP	5.5[a]
FPL + 10 ppm NTMP	37[c]
FPL + 10 ppm PA	18[c]

[a] Determined by visual observation

[b] Sample had not hydrated after 5 days

[c] Determined by ellipsometry
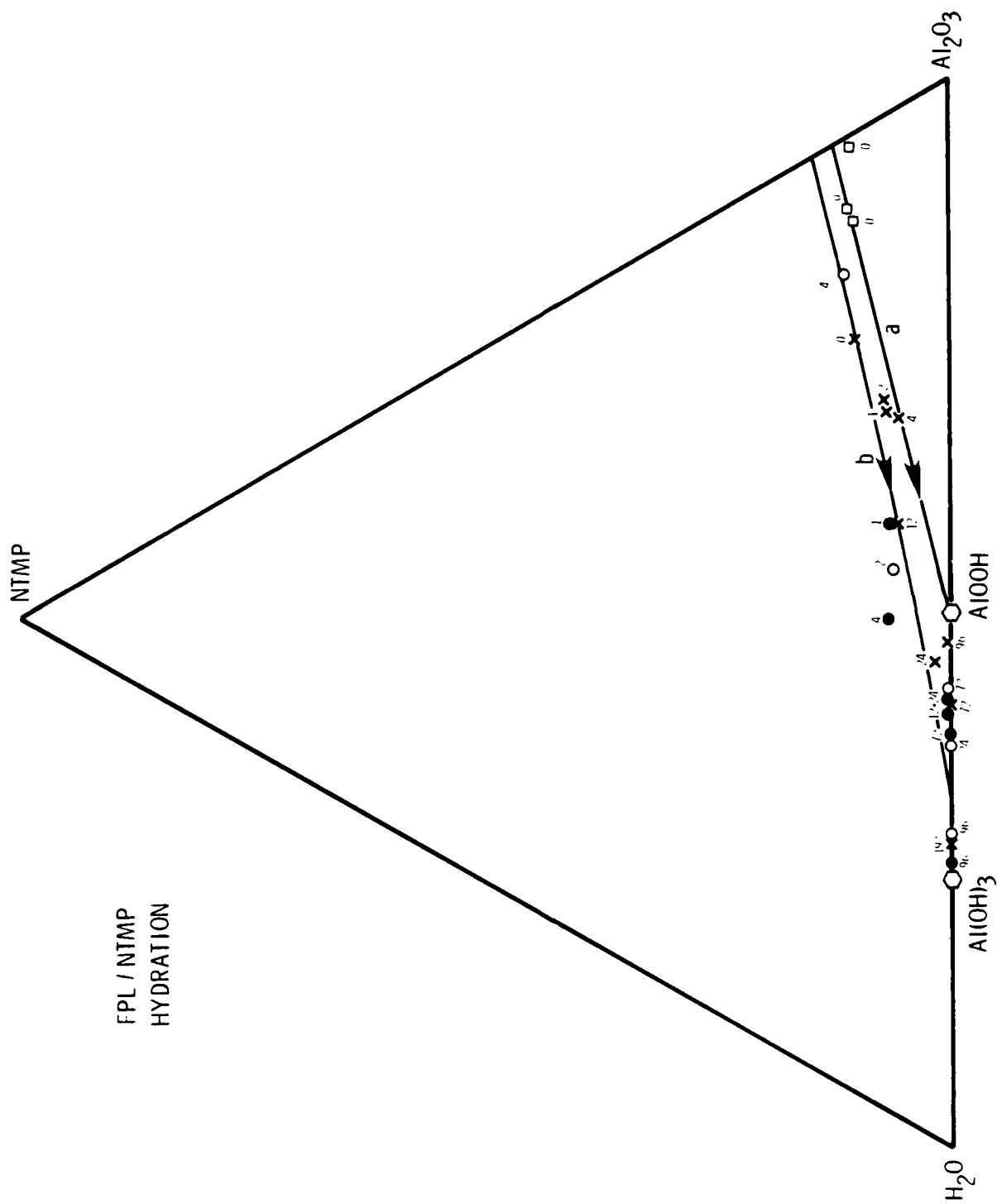
Figure 9. Al_2O_3–NTMP–H_2O SBD showing the evolution of FPL-etched surfaces treated with saturation coverages of NTMP, as a function of exposure time in 100% relative humidity at 50°C. The different symbols represent different experimental runs; the numbers are the exposure time in hours.[15]

(UHV), so that their final composition was near line a. Finally, Auger depth profiles of several hydrated samples revealed no subsurface concentration of phosphorus for coupons without surface phosphorus.

Similar behavior upon hydration was also observed for FPL surfaces treated with (n Bu)NBMP. The surface again evolved directly from Al_2O_3 with a monolayer of inhibitor, to AlOOH, and then to $Al(OH)_3$.

2. Mechanical Testing

a. Initial Bond Strengths

The initial dry strength of treated structures was compared with that of control structures using a variety of adhesives in T-peel and double-lap-shear tests to determine the compatibility of different adhesive-inhibitor systems. The T-peel strength values are given in Table IV. For most adhesives, three classes of inhibitors were tested: NTMP, our standard compound; (n Bu) NBMP, which has an exposed inert hydrocarbon chain; and MP, the simplest phosphonic acid. For each of the epoxy adhesives tested, the treated structures, including those with supermonolayer coverages of inhibitors, exhibited the same pull strengths as the control FPL structures, indicating no degradation of the dry interfacial strength. In fact, failure of the specimens examined by XPS occurred cohesively in the adhesive as shown by the high C and low O concentrations of each side (Table V). Such a failure mode represents the best performance of any given adhesive structure and indicates that the "weakest link" of the system is the strength of the polymer. The behavior of the samples bonded with a nitrile phenolic is different. For unprimed structures (a procedure not recommended with FM 238), a significant degradation of pull strength occurred upon inhibitor treatment, especially with (n Bu)NBMP. For primed structures, only a slight degradation was measured. Failure in both cases occurred within the polymeric material, suggesting that the inhibitor may have weakened the unprimed adhesive, perhaps by interfering with the cure or by modifying its wetting ability.

Table IV

T-peel Strengths for FPL-Etched Adherends

Adhesives

Treatment	FM-123-5 Nitrile Epoxy	FM 238[a] Nitrile Phenolic	FM 238/BR238[b] Nitrile Phenolic	FM1000 Polyamide Epoxy	FM 53 Epoxy
Control	172 ± 26 kPa	201 ± 23 kPa	259 ± 21 kPa	554 ± 13 kPa	351 ± 32 kPa
MP 300 ppm	152 ± 16	120 ± 18	201 ± 18	----	----
NTMP					
10 ppm, RT	225 ± 23	145 ± 20	195 ± 11	576 ± 11	350 ± 54
100 ppm, RT	164 ± 6	108 ± 19	164 ± 6	550 ± 6	353 ± 36
100 ppm, 80°C	156 ± 10	54 ± 12	204 ± 21	576 ± 0	----
(n Bu)NBMP					
10 ppm. RT	161 ± 6	c	241 ± 11	569 ± 8	----
100 ppm, RT	165 ± 12	<34	185 ± 18	569 ± 8	----
100 ppm, 80°C	159 ± 14	<34	169 ± 7.6	576 ± 0	----
Failure-Visual	Cohesive	Adhesive	Adhesive[d]	Cohesive/Adhesive	Cohesive
XPS	----	Cohesive	Cohesive	Cohesive	----

a Not primed

b Primed with BR 238

c 2 samples averaged 95 kPa, 4 samples 34 kPa

d Between primer and adhesive

Table V

Surface Composition of Adjoining T-peel Surfaces for FPL-etched Adherends

Composition (at. %)

Adhesive	Inhibitor	Al		O		C		Other		Failure Mode
		M[a]	A[a]	M[a]	A[a]	M[a]	A[a]	M[a]	A[a]	
FM238	Control	0	0	6.6	4.5	87.0	87.4	N = 6.4	S = 0.4 N = 7.6	Cohesive
FM238	NTMP 100 ppm	0	0	8.6	4.5	86.8	88.0	N = 4.6	N = 6.0 Si = 1.5	Cohesive
FM238	(n Bu)NBMP 100 ppm, RT	4.9	3.1	17.2	10.0	78.0	84.3	---	Si = 2.5	Cohesive
FM238/BR238	Control	0	0	11.0	8.3	77.6	82.1	N = 4.0 Si = 7.3	N = 5.2 Si = 4.4	Cohesive[b]
FM238/BR238	NTMP 100 ppm, RT	1.7	0	12.2	9.1	79.0	78.7	N = 4.7 Si = 2.4	N = 5.6 S = 6.3 Si = 6.3	Cohesive[b]
FM238/BR238	(n Bu)NBMP 100 ppm, RT	0	0	9.7	11.2	80.9	76.6	S = 0.4 N = 3.9 Si = 5.0	N = 4.7 Si = 7.5	Cohesive[b]
FM1000EPI5	Control	1.1	0.6	18.5	14.3	70.8	75.4	N = 5.7 Si = 3.9	N = 8.7 Si = 1.0	Cohesive
FM1000EPI5	NTMP 100 ppm, RT	1.2	0	22.3	18.1	66.1	73.9	N = 3.9 Si = 6.5	N = 7.0 Si = 1.1	Cohesive
FM1000EPI5	(n Bu)NBMP 100 ppm, RT	2.6	0	20.6	14.4	68.3	75.3	N = 5.4 Si = 3.1	N = 7.6 Si = 2.7	Cohesive

a M = metal side; A = adhesive side
b Cohesive with primer/adhesive system

The double lap shear results, shown in Table VI, gave very similar results for two epoxy adhesives, including one cured at room temperature. No degradation (or enhancement) of the dry strength was seen following NTMP treatment.

b. Bond Durability in Moist Environments

Testing the inhibitors' effectiveness in promoting bond durability has largely involved wedge tests; however, a few double-lap-shear specimens were exposed to high humidity for seven days. The lap shear results, shown in Table VII, indicate that some degradation of the bond strength has occurred relative to the initial strengths (Table VI). In most cases, the bond strengths of treated specimens approach, but are less than, the values for the control specimens. The inhibitors' effectiveness in increasing hydration resistance is not evident here because failure occurred cohesively within the adhesive instead of interfacially.

Wedge tests measurements are a more severe test of interfacial stability and have been used extensively both to study the mechanisms of crack propagation and to evaluate the effectiveness of the different inhibitors. Typical wedge-test data for our FPL adherends treated in room-temperature NTMP solutions are shown in Fig. 10. The NTMP significantly improved the durability of the FPL-etched adherends over that exhibited by untreated adherends. Indeed, the performance of the FPL adherend treated in the NTMP solution approached that of the PAA adherends and is typical of FPL adherends treated in NTMP solutions of 10-500 ppm. Occasionally, the performance of specimens treated in 10 ppm NTMP solutions was not as good. We attribute this variability to scatter in the surface coverage from solutions near the "knee" of Fig. 4. Wedge-test results obtained using FPL adherends treated with 10 ppm NTMP solutions at 80°C (Fig. 11) show nearly the same performance as adherends treated at room temperature despite an increase in the NTMP coverage of ~2-3 times the room-temperature value.

Table VI

Double-Lap-Shear Initial Strengths for FPL-etched Adherends

Sample Description	Adhesives	
	FM 123-2	Cybond 1102
Control	27 MPa	18 MPa
NTMP 100 ppm, RT	27 MPa	19 MPa
Failure, visual	Cohesive	Cohesive/adhesive

Table VII

Double Lap Shear Strengths for FPL-Etched Adherends
After Exposure to High Humidity

Treatment	Adhesives	
	FM 123-2	Cybond 1102
Control	22 MPa	13.1 MPa
NTMP, 100 ppm, RT	21	11.7
(n Bu)NBMP, 100 ppm, RT	23	10.0
MP, 100 ppm, RT	19	11.4
Failure, visual	Cohesive for all cases	Cohesive for all cases
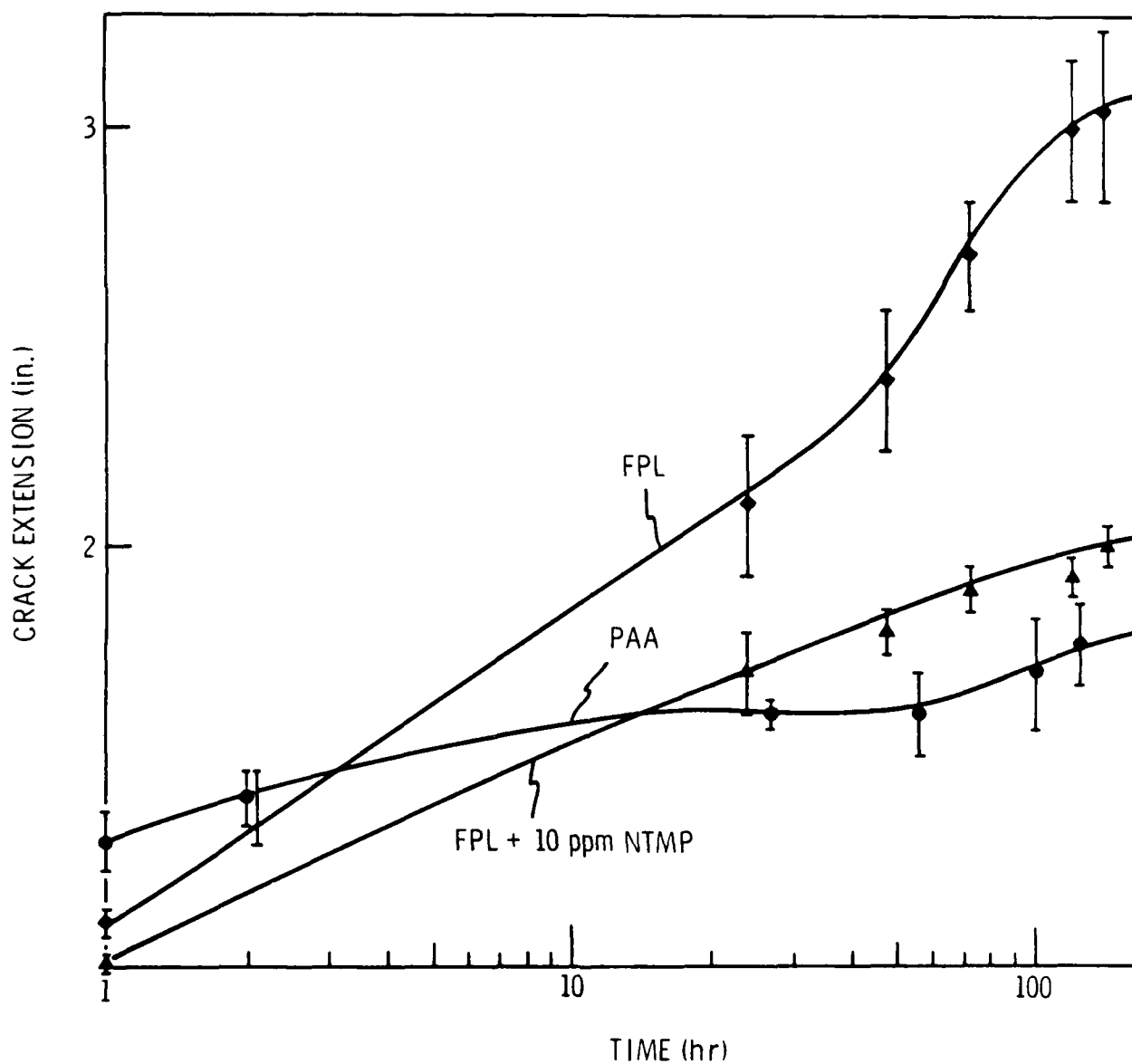
Figure 10. Wedge test results (crack length as a function of time) for FPL, NTMP-treated FPL, and PAA adherends treated at room temperature.[11]
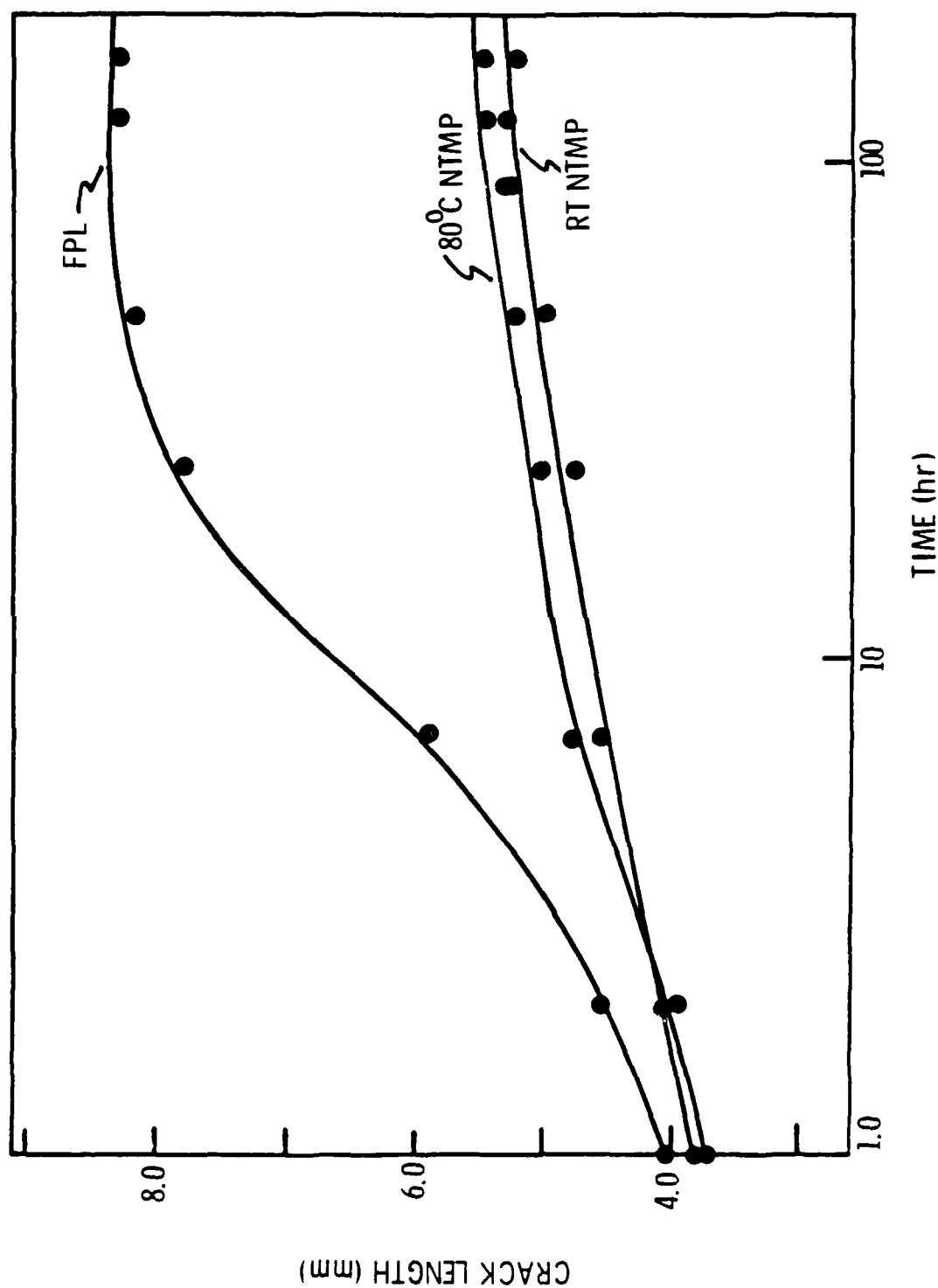
Figure 11. Wedge test results (crack length as a function of time) for FPL-
and NTMP-treated FPL adherends treated at room temperature and at
80°C. NTMP solution concentration was 10 ppm.[11]

Using the crack-length data generated by the wedge-tests and Eq. 1, we calculated the fracture energy, G. The crack velocity, v, was determined graphically from plots of crack length as a function of time; it is shown as a function of G in Figs. 12 and 13. The fracture energy analysis allows further evaluation of the inhibitor surface treatments with calculation of G_I values (Table VIII). G_I is the value of G where crack propagation is below the level of experimental detectability. The significance of these results will be discussed below. At the conclusion of the humidity exposure, the wedge-test assemblies were separated. We observed that the original crack through the adhesive did not continue to propagate* after exposure to humidity. Instead, a new crack initiated at the oxide/adhesive interface and continued at this location until crack arrest. Figure 14 is a low-magnification SEM micrograph of this initiation region. The raised adhesive indicates that the adhesive layer remained in one piece until separation of the adherends caused it to rupture. The mechanism of crack propagation will be discussed in the final section.

The other principal use of the wedge test was to evaluate the effectiveness of the various inhibitors shown in Figs. 1 and 2 in improving bond durability.

Based on the results shown in Figs. 15-17, we classified the inhibitors into three groups: (I) MP and PA, which provide either worse performance or no improvement over the untreated FPL specimens; (II) AMP and (t Bu)NBMP, which provide some improvement over the control; and (III) NTMP, (nBu) NBMP, and EDTMP, which provide the best performances.

To determine the microscopic locus of failure of the wedge-test specimens, we obtained X-SEM micrographs and/or XPS measurements of the near-

---

* In the absence of high humidity, the original crack did not propagate even at 60°C.
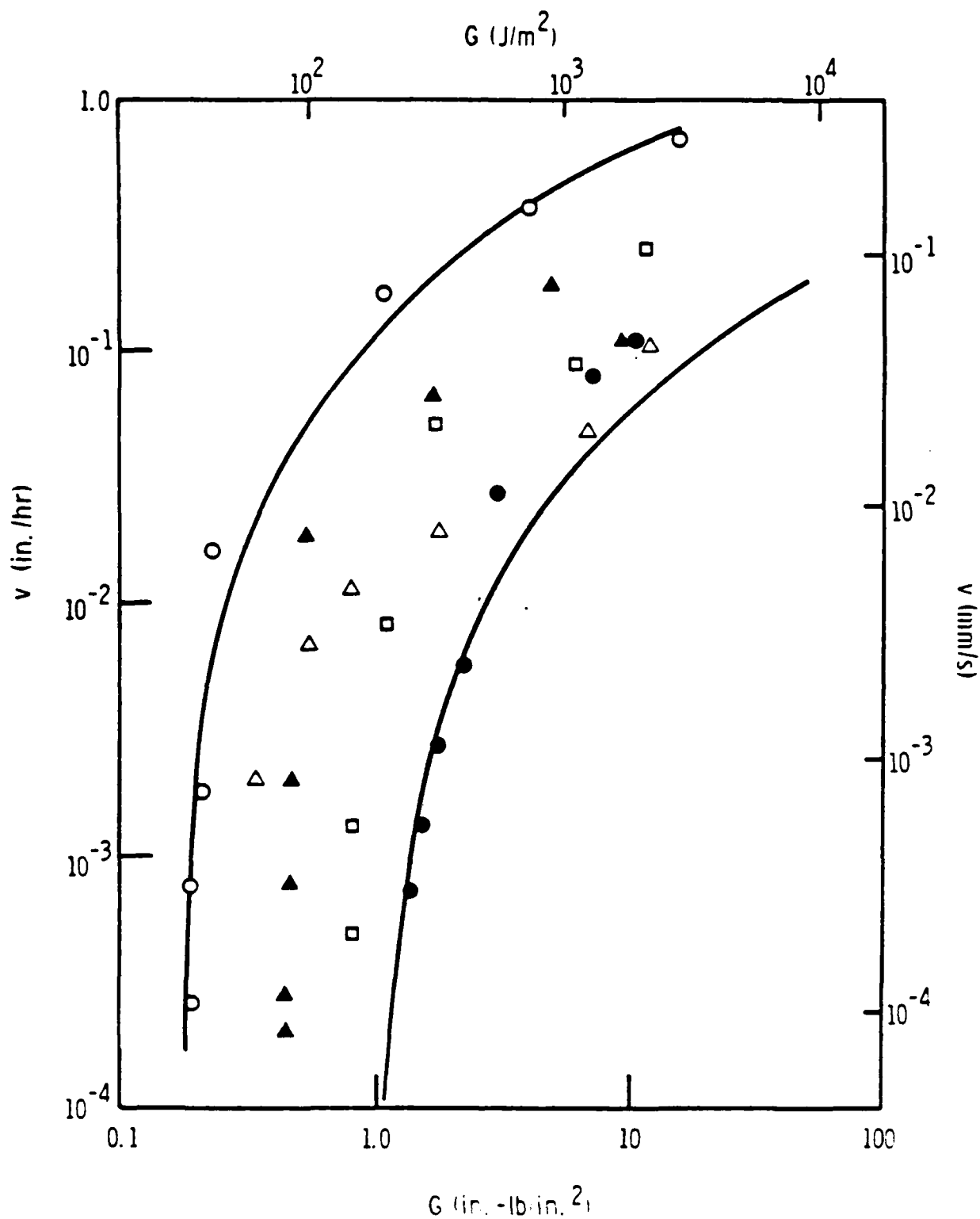
Figure 12. Wedge test results (crack velocity as a function of fracture energy) for untreated FPL adherends.[14]
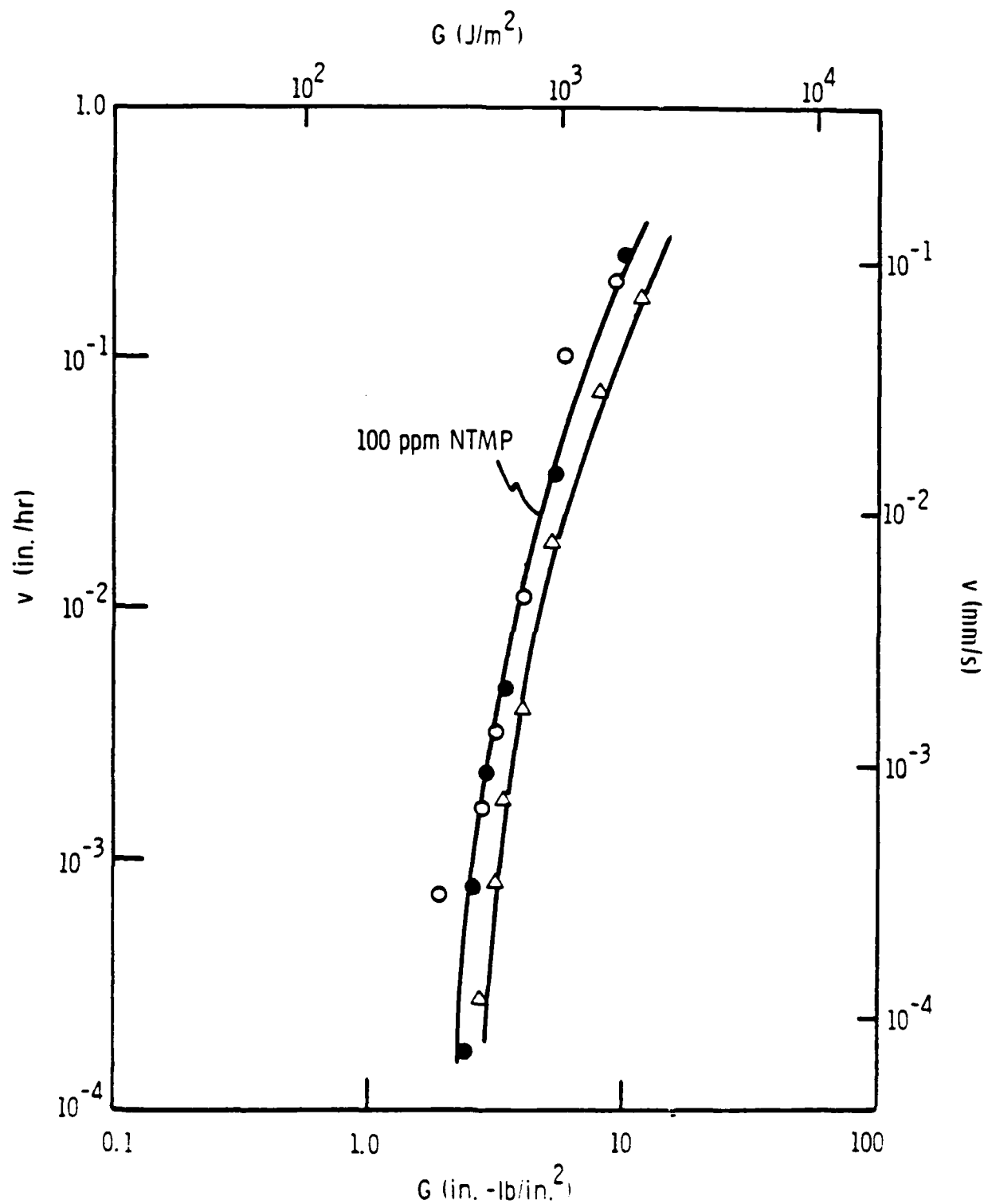
Figure 13. Wedge test results (crack velocity as a function of fracture energy) for FPL adherends treated in 100-ppm NTMP solutions.[14]

Table VIII

G_I Obtained from Wedge Tests of FPL-etched adherends

Sample Description	G_I (J/m^2)
Control	35–175
2 ppm NTMP, RT ⎱ 10 ppm NTMP, RT ⎰	105–440
100 ppm NTMP, RT	350–525
Adhesive	1,140
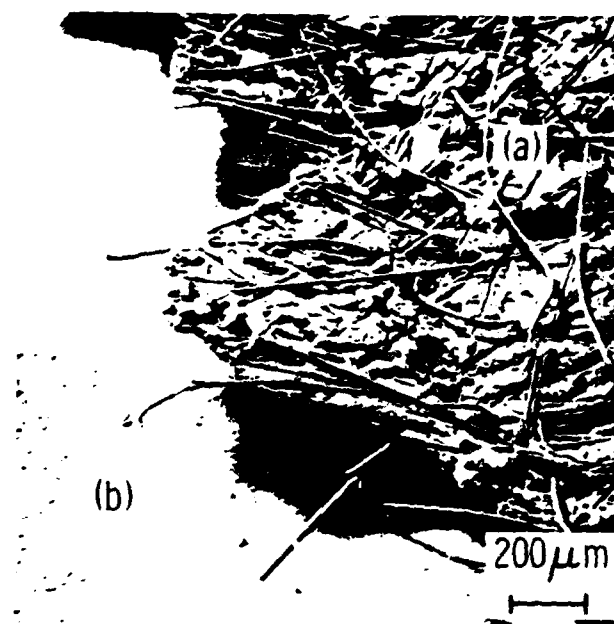
Figure 14. Scanning electron micrograph of fracture surface at the position where stress concentration caused by crack in adhesive (a) initiates an interfacial failure (b). Arrow indicates initiation site of interfacial crack. [14]
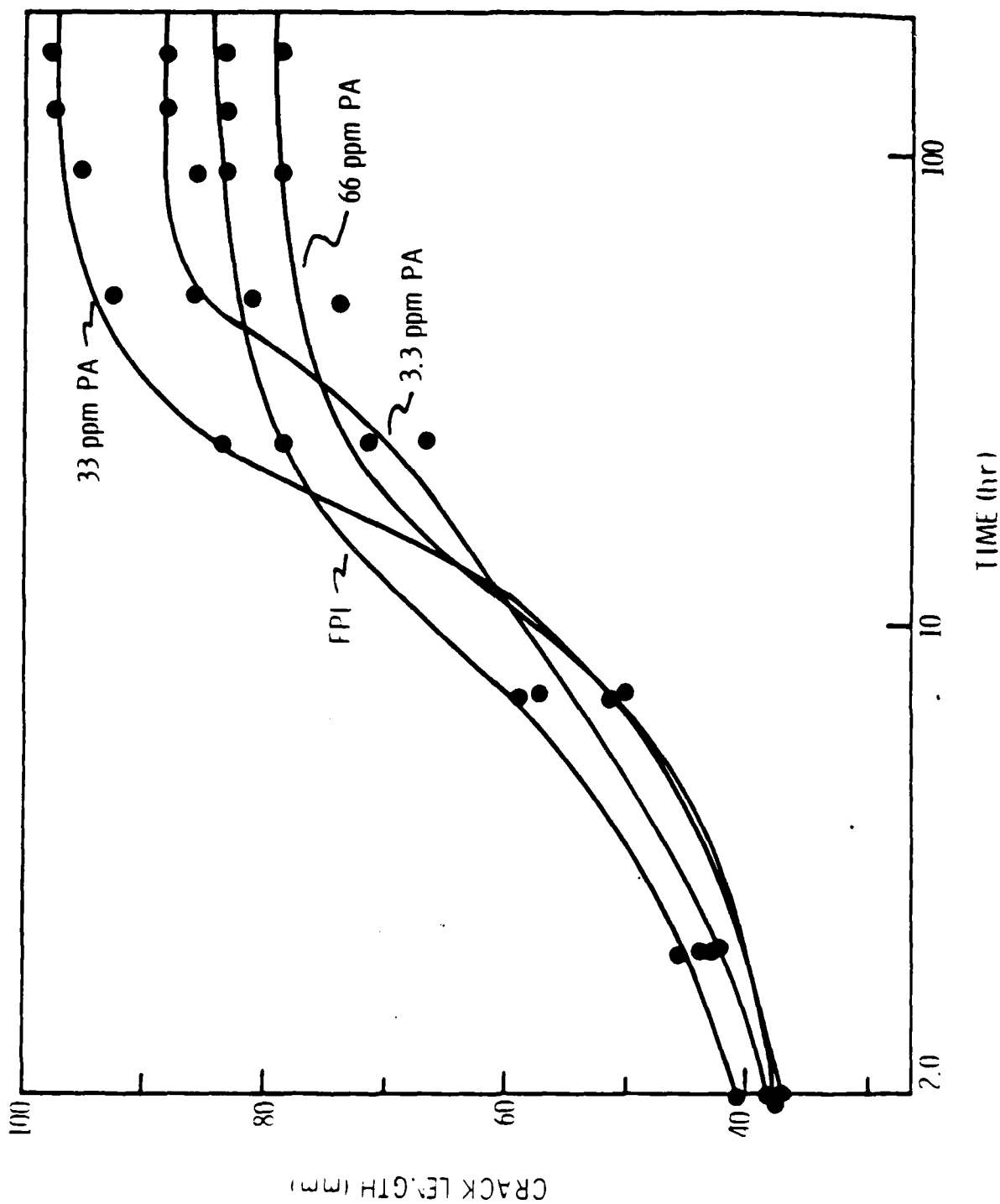
Figure 15. Wedge-test results (crack length as a function of time) for FPL adherends treated in solutions of PA and for untreated FPL adherends. [14]

Figure 16. Wedge-test results (crack length as a function of time) for untreated FPL adherends and for FPL adherends treated in MP, AMP, (n Bu)NBMP, and NTMP solutions.[17]

Figure 17. Wedge-test results (crack length as a function of time) for untreated FPL adherends and for FPL adherends treated in AMP, (n Bu)NBMP, NTMP, and EDTMP solutions.[17]

crack-tip region for selected samples in each of the three groups. The XPS results are summarized in Table IX. The failures of MP-, PA(66 ppm)-, NTMP- (both 100 ppm at room temperature and 10 ppm at 80°C), and EDTMP-treated specimens occur near or at the adhesive-adherend interface because substantial differences are seen between the metal and adhesive sides of the failure. In such cases, Al (and O) denotes aluminum oxide or hydroxide and high C denotes the adhesive. [Al and some O on the adhesive side of NTMP- and EDTMP-treated bonds result from aluminum hydroxides that are solution-deposited from the condensed water vapor. Similarly the C on the metal side results from adventitious hydrocarbon contamination.] In contrast, the two surfaces of the FPL control and specimens treated with (t Bu)NBMP and (n Bu)NBMP exhibit high Al and O and low C, indicating that the locus of failure is in the oxide/ hydroxide or at the interface between the oxide/hydroxide and the metal, with subsequent hydration or corrosion of the metal surface.

In most specimens that show improvement over the control, bond failure occurred as a result of hydration of the adherend surface. For example, panels treated with AMP and (nBu)NBMP exhibit the cornflake morphology of boehmite up to the crack-tip (Fig. 18). More extensive hydration, i.e., bayerite crystallites on top of the boehmite, is also seen in some areas.

In contrast, visual observations of the near-crack-tip region of NTMP- treated panels reveal a "shiny" aluminum area right at the crack tip and a "dull" region further along the crack (Fig. 19). Upon closer examination, the shiny area exhibits an FPL morphology, whereas the dull area exhibits the cornflake morphology. In this case, the crack apparently has propagated in advance of the hydration of the aluminum oxide; only after additional exposure to the moist environment does hydration occur.

Using these results and what is mentioned in the discussion presented in Section IV, we subsequently designed, synthesized, and tested three additional inhibitors (Fig. 2): (r Bu)ANBMP, which is an analog of (n Bu)NBMP that can chemically react with an epoxy adhesive, and 2ϕ and 2pA, which are an

Table IX

XPS Surface Composition of Wedge Tested FPL Adherends
Pretreated with Various Inhibitors

Composition (at. %)

Group	Sample Description	Al M^a	Al A^b	O M^a	O A^b	C M^a	C A^b
	Adhesive	--	0	--	8	--	92
	Control	22	24	44	47	34	30
I	MP, 300 ppm	20	0	50	21	29	78
I	PA, 3.3 ppm	18	15	46	43	36	42
I	PA, 33 ppm	17	17	52	42	21	41
I	PA, 66 ppm^c	25	2	49	25	25	73
II	(t Bu)NBMP, 300 ppm	30	29	59	58	10	12
III	NTMP, 100 ppm, RT	30	14	56	38	13	47
III	NTMP, 10 ppm, 80°C	14	2.5	40	25	45	72
III	EDTMP, 300 ppm	29	19	59	45	12	36
III	(n Bu)NBMP, 300 ppm	31	30	56	58	13	11

[a] metal side

[b] adhesive side

[c] P also detected
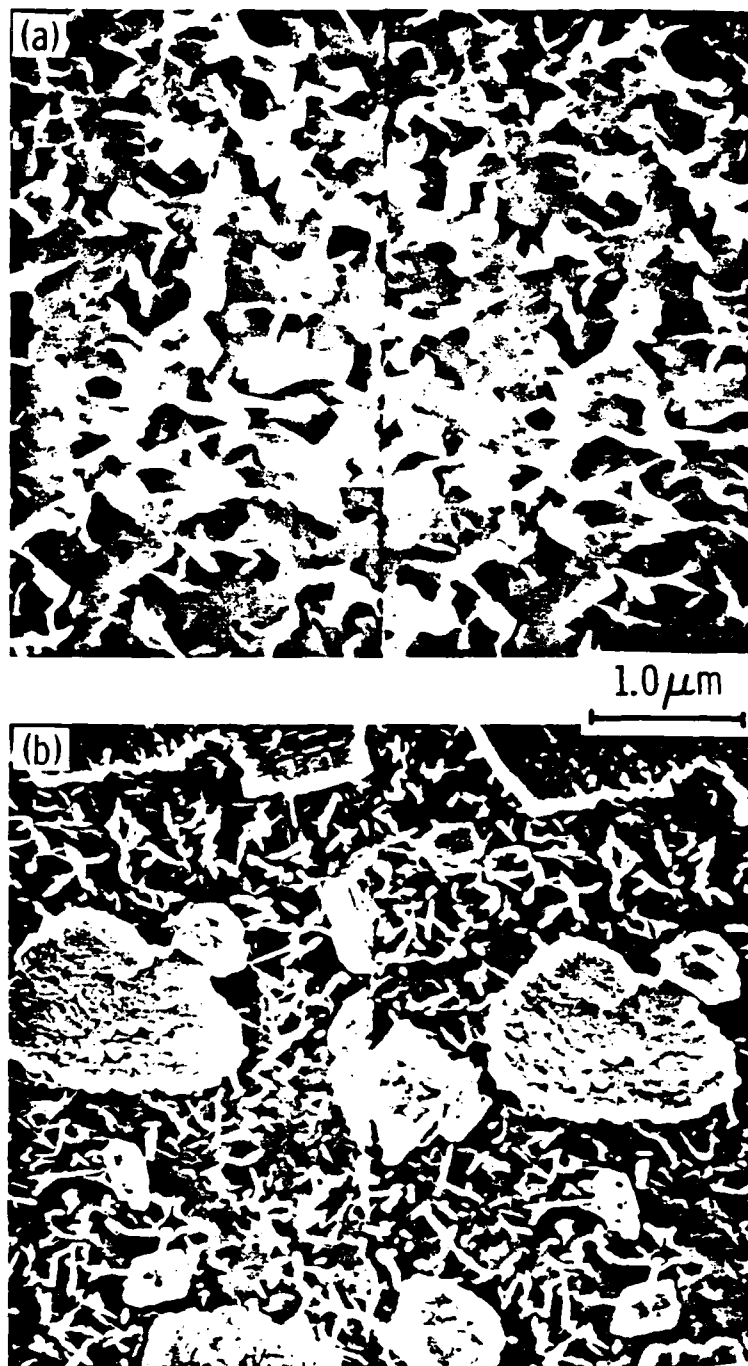
Figure 18. Scanning electron micrographs of the near-crack-tip region of the aluminum side of two inhibitor-treated FPL-etched wedge-test specimens: a) AMP-treated surface exhibiting cornflake (boehmite) morphology and b) (n Bu)NBMP-treated surfaces exhibiting bayerite crystallites on top of boehmite.[17]

-41-
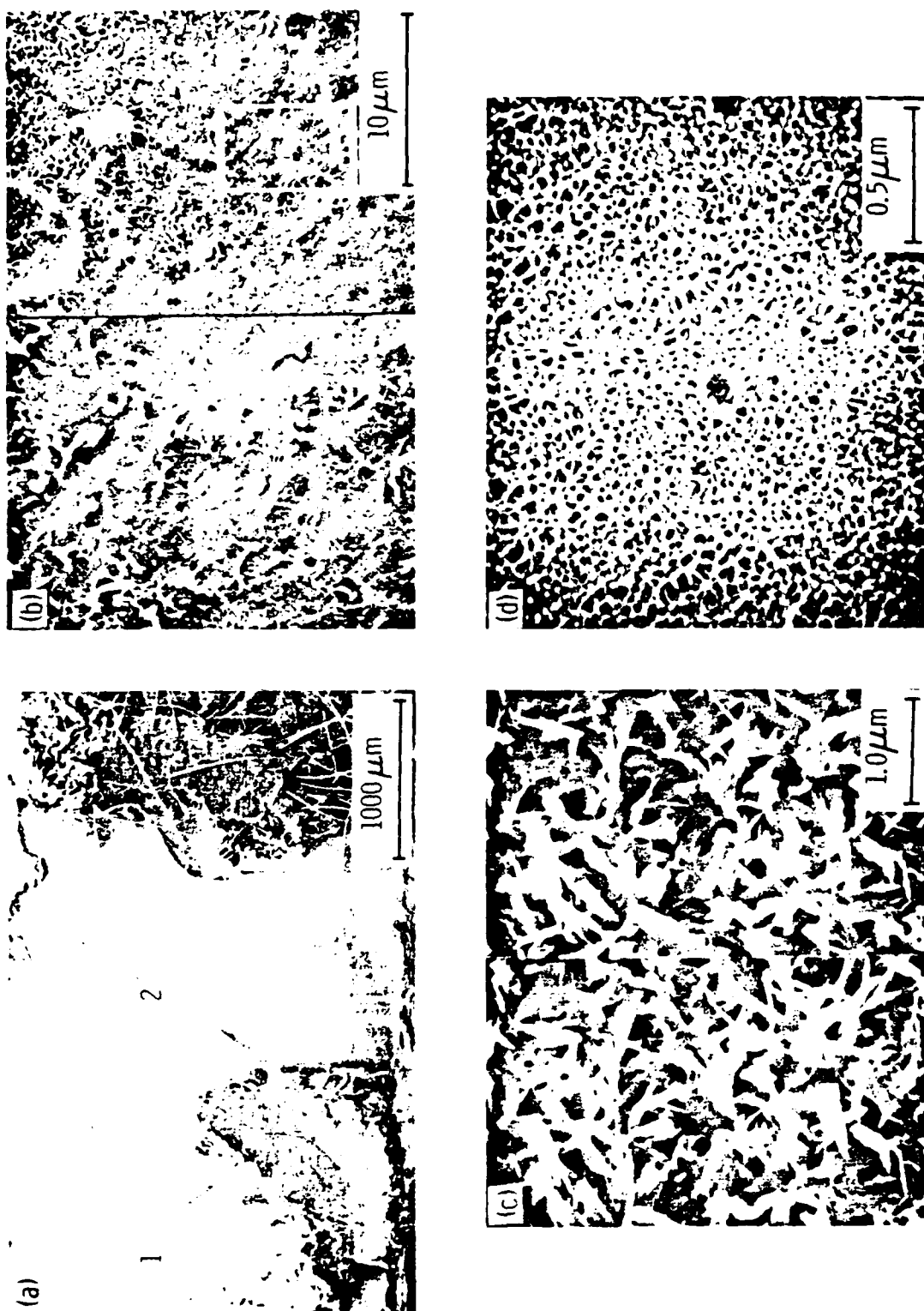
Figure 19. Scanning electron micrographs of the near-crack-tip region of the aluminum side of an NTMP-treated FPL-etched wedge test specimen: a) low magnification view showing 1) the dull aluminum area and 2) the shiny aluminum area, and the cohesive failure in the adhesive after the wedge test was completed (at right); b) the beginning of hydration in the boundary region between dull and shiny areas, enlargment of the blocked-in area is at left; c) higher magnification stereo view of the dull area showing the corn-flake boehmite structure; and d) high-magnification $5\{\frac{+5}{-5}\}0$ view of the shiny area showing the original FPL morphology.[17]

inert/reactive pair similar to EDTMP. In wedge-tests using these and some of the earlier compounds (Fig. 20), four of the inhibitors showed equivalent performance over the best NTMP-treated structures. [The performance of the NTMP-treated structures in this particular test was at the extreme of the scatter band observed for such samples.] Macroscopically, failure occurred interfacially.

B. PHOSPHORIC-ACID-ANODIZED SURFACES

1. Surface Chemistry-NTMP Adsorption

The inhibitor surface coverage (P/Al ratio) on PAA oxide surfaces as a function of NTMP solution concentration saturates at solution concentrations above 10 ppm (Fig. 21) much like that on FPL oxide surfaces. Even though the P/Al ratio of the untreated PAA oxide is 0.1 compared with zero for an FPL oxide, both oxides have P/Al ratios of 0.15-0.20 following saturation treatment at room temperature. This similarity is duplicated in the 80°C treatment, i.e., at a solution concentration of 300 ppm, the P/Al ratio for both FPL and PAA oxides ranges from 0.4-0.5, which corresponds to multilayer surface coverages. Upon adsorption, however, the surface chemistry behavior of FPL and PAA oxides differs dramatically, as illustrated by the SBD of Fig. 22. Because the initial PAA surface contains very little adsorbed water for the NTMP to displace,[20] adsorption is a simple addition reaction, with the PAA surface composition evolving along a line drawn to the NTMP composition point.

2. Mechanical Testing of Bond Durability in Moist Environments

Wedge-tests (Fig. 23) using PAA adherends demonstrate that the bond durability of these adherends is better than that of FPL adherends and can be further improved by NTMP pretreatment. This performance is independent of treatment solution concentration provided room-temperature saturation coverage is obtained.[18] However, at higher coverages (achieved at elevated
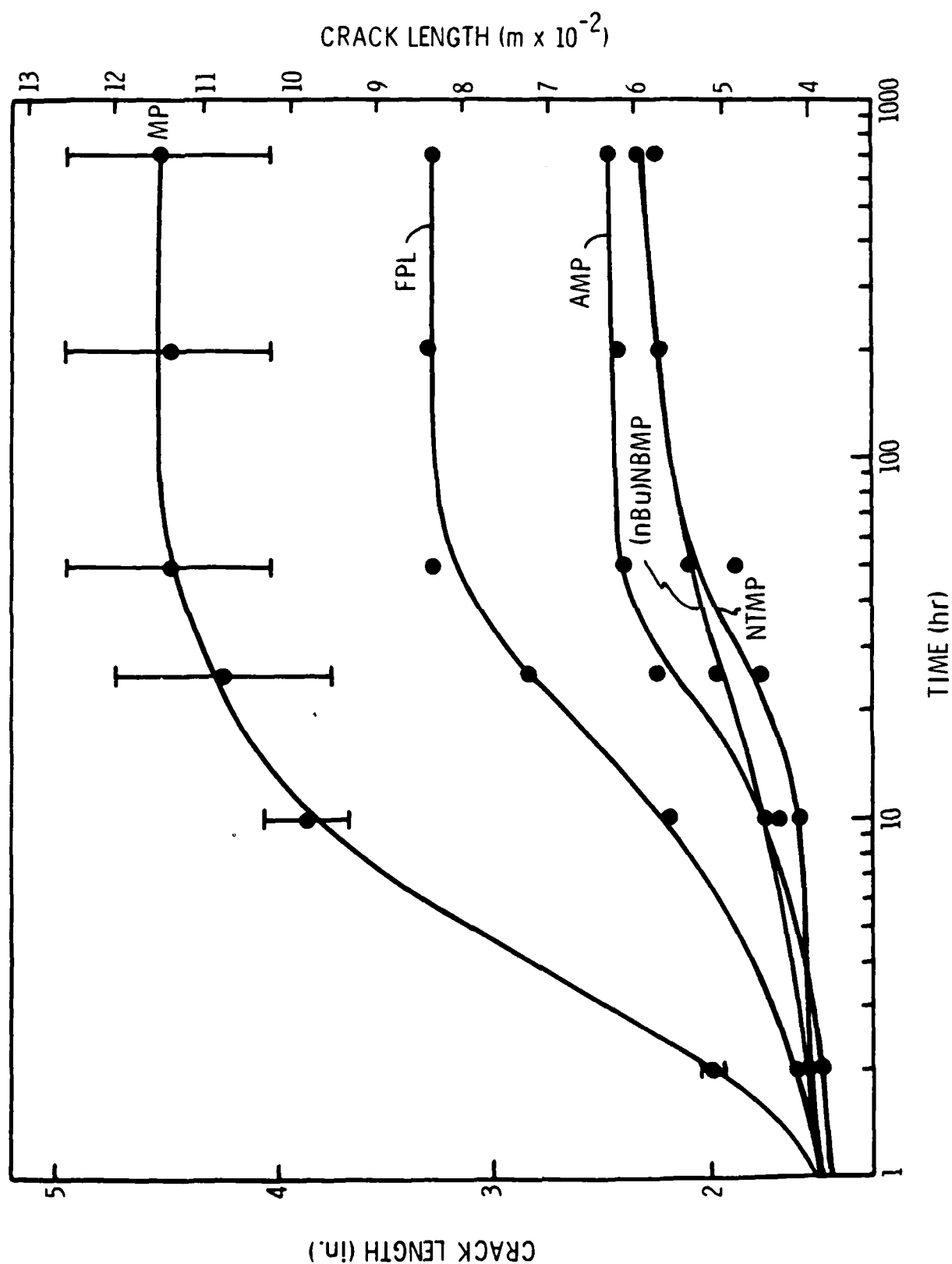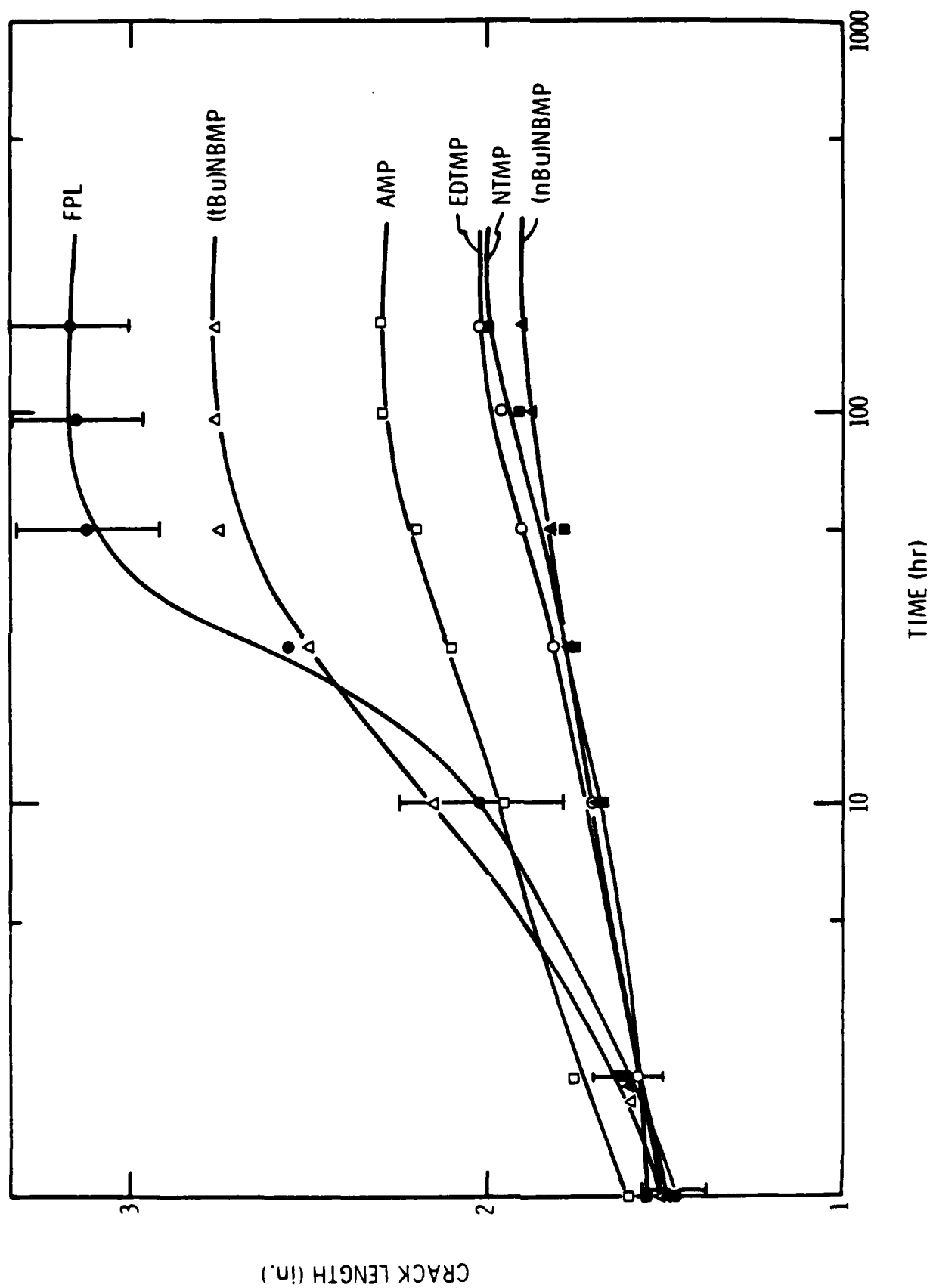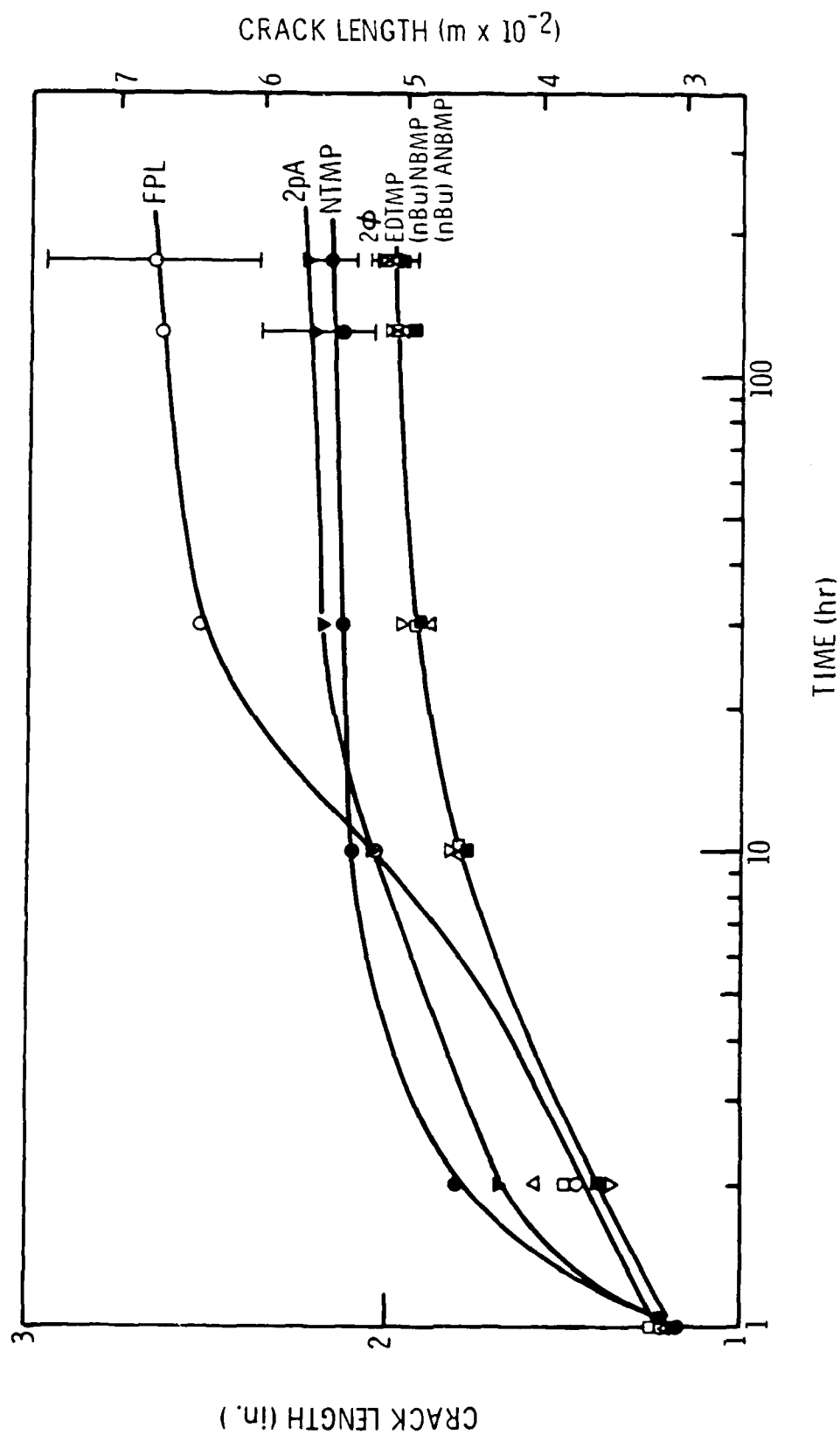
Figure 20). Wedge-test results (crack length as a function of time) for untreated FPL adherends and for FPL adherends treated in solutions of 2pA, NTMP, 2ɸ, EDTMP, (n Bu)NBMP, and (n Bu)ANBMP. [10]
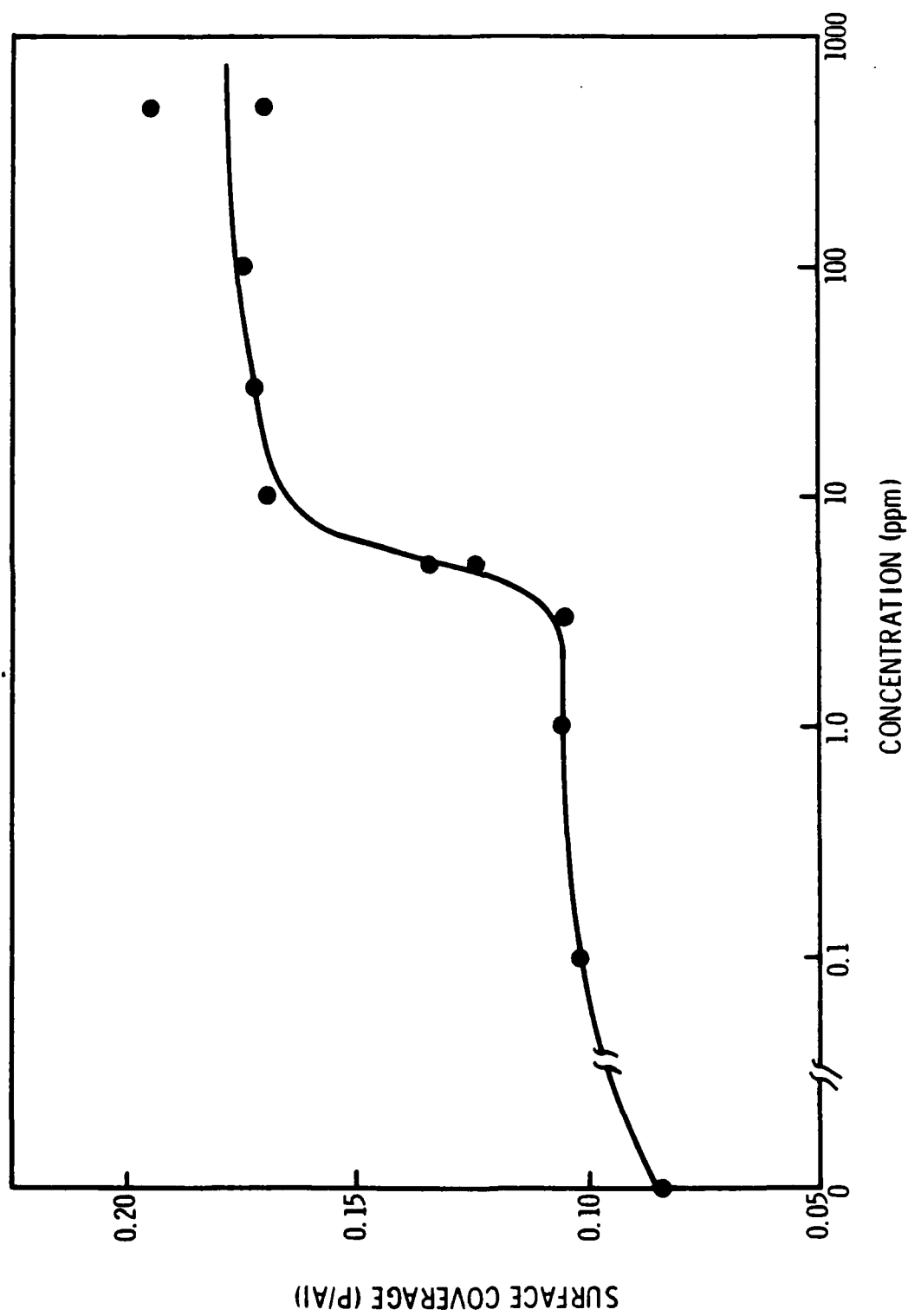
Figure 21. Surface coverage of NTMP-treated PAA oxide surfaces (P/Al) as a function of NTMP solution concentration.[18]
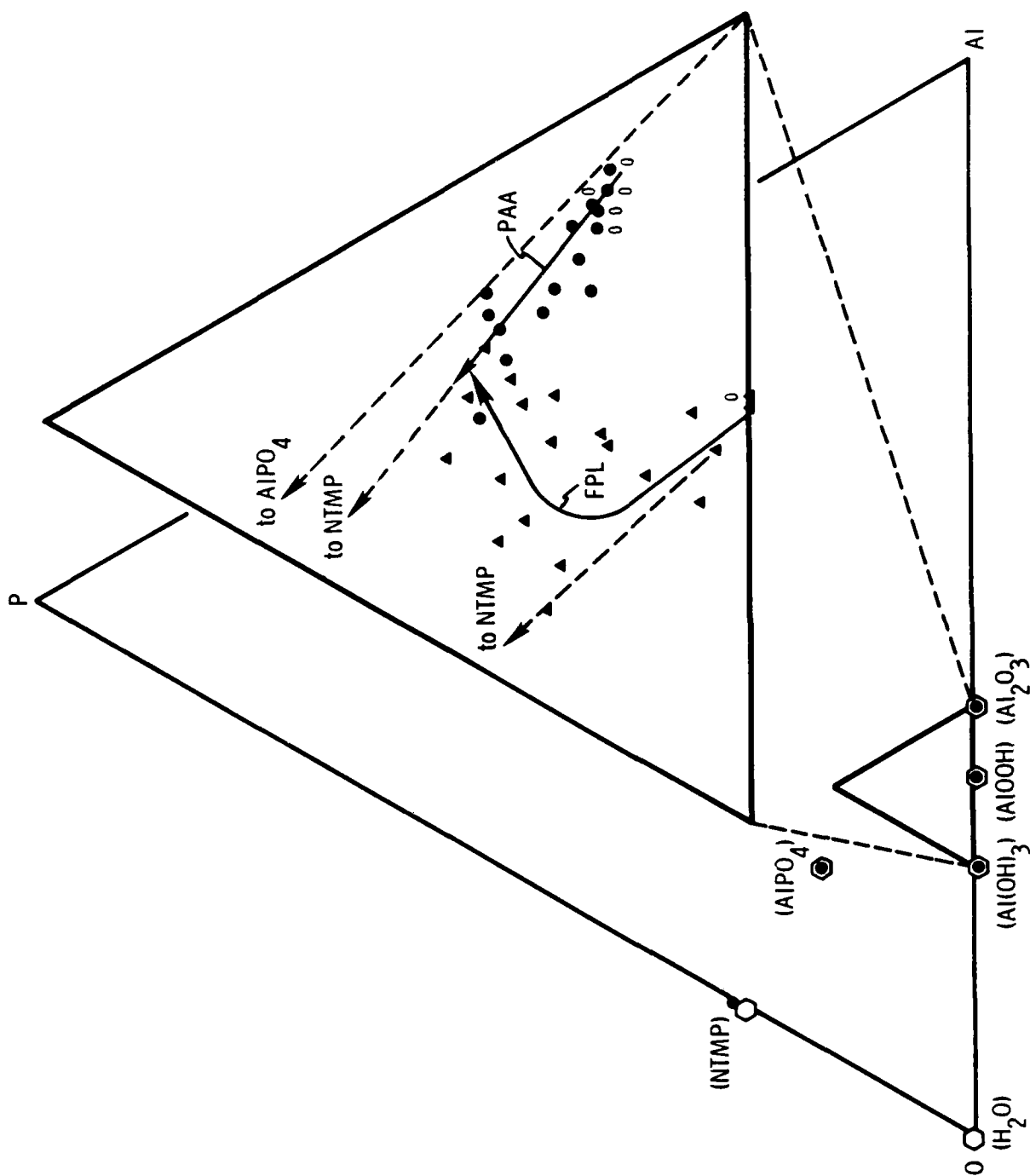
Figure 22. Al-P-O SBD showing the surface composition of FPL-etched surfaces (triangles) and PAA-treated surface (circles) after immersion in various concentrations of NTMP solution. Open hexagons are calculated compositions. Closed symbols are measured compositions. Compositions depicted by "O" represent surfaces not immersed in NTMP solutions.[15]
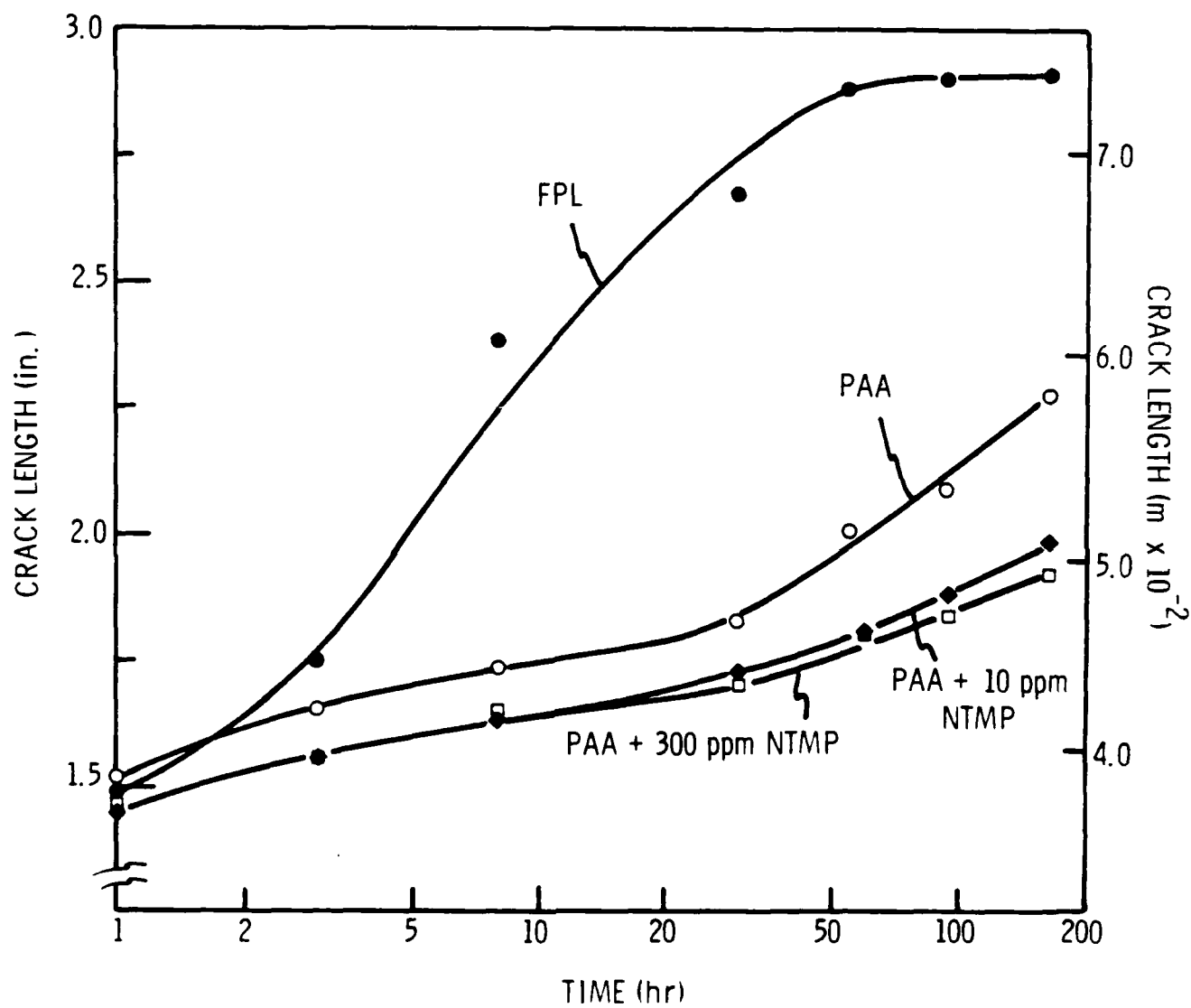
Figure 23. Wedge test results (crack length as a function of time) for untreated FPL and PAA adherends and PAA adherends treated with 10-ppm and 300-ppm NTMP solutions.[18]

temperature), bond durability can be reduced relative to that provided by room-temperature treatment (Fig. 24).

Crack extension forces and resultant crack velocities were derived from the wedge-test results using Eq. 1 (Figs. 25 and 26). Data for the adhesive FM 123-2, which were obtained using PAA-adherends sprayed with a corrosion-inhibiting primer prior to bonding, are also included. Because the crack was completely cohesive through the center of the adhesive layer in this case, the wedge test provided information on the fracture behavior of the adhesive alone when bonded to PAA adherends. Following the humidity exposure, the wedge-test assemblies were separated. As shown earlier for FPL adherends, X-SEM examination (Fig. 27) confirmed that establishment of a warm humid environment at the crack tip always initiated a new crack at the oxide/adhesive interface, even on inhibitor-treated PAA adherends. The re-initiation and initial propagation of the crack was associated with conversion of the original oxide to boehmite.

Visual examination of the adherends (with or without inhibitor treatment) indicated that the crack path was not confined exclusively to one oxide/adhesive interface. Furthermore, the failure surface on the aluminum side was dull or stained where the inital crack propagated, but was shiny and had a slight purple sheen near the final crack tip. On the adherends treated in high concentration (200-500 ppm) NTMP solutions and in 80°C solutions, the final increment of crack extension often consisted of regions where crack propagation had occurred wholly within the adhesive layer. X-SEM examination of the Al side of the fracture surface revealed that the dull regions corresponded to a hydrated surface, and the shiny regions corresponded to an oxide surface coated with a thin adhesive layer; the transistion from dull to shiny corresponded to the horizontal portion of the crack length vs time curves of Fig. 23. Figure 27a is a schematic view of the overall surface. The surface away from the crack tip had the cornflake morphology of boehmite as shown in Fig. 27b, whereas the surface at the crack tip exhibited the morphology of failed adhesive (Fig. 27c). Since there was no evidence of the Dacron mat on the failure surfaces, the crack evidently progressed in the
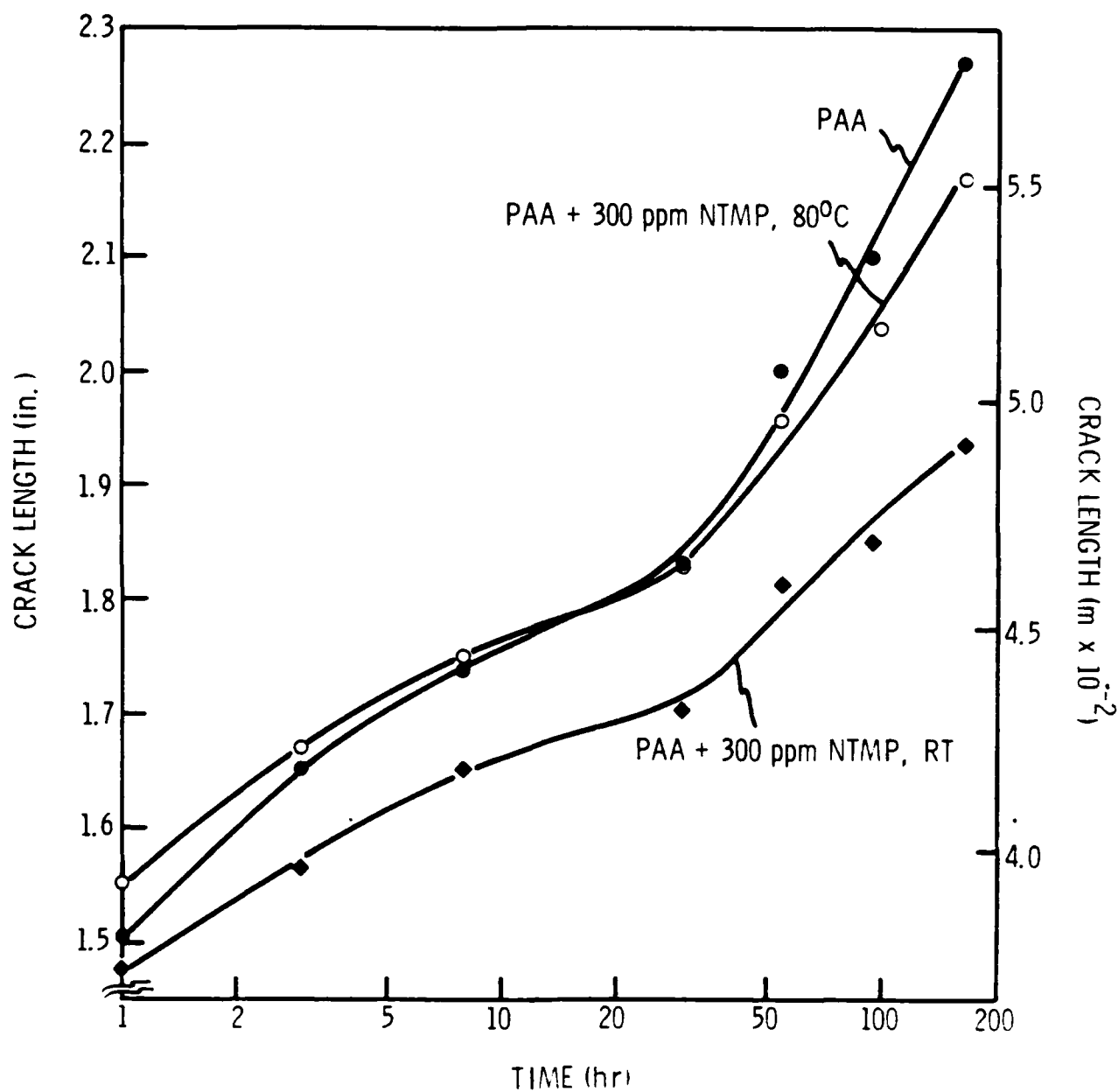
Figure 24. Wedge test results (crack length as a function of time) for untreated PAA adherends and PAA adherends treated in 300-ppm NTMP solutions at either room temperature or 80°C.[18]

-49-
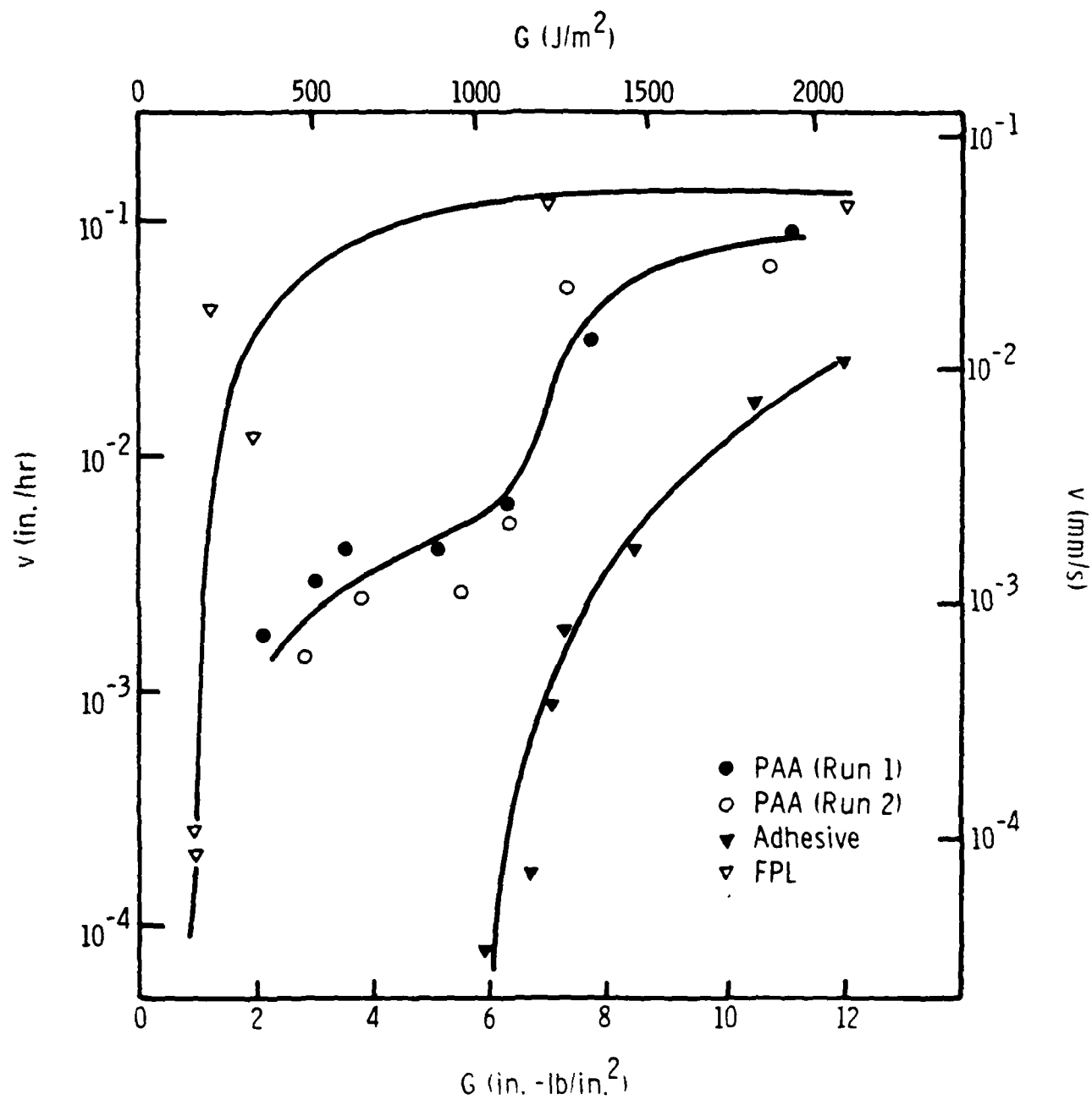
Figure 25. Wedge test results (crack velocity as a function of fracture energy) for untreated FPL, PAA, and FM 123-2 adhesive.[18]
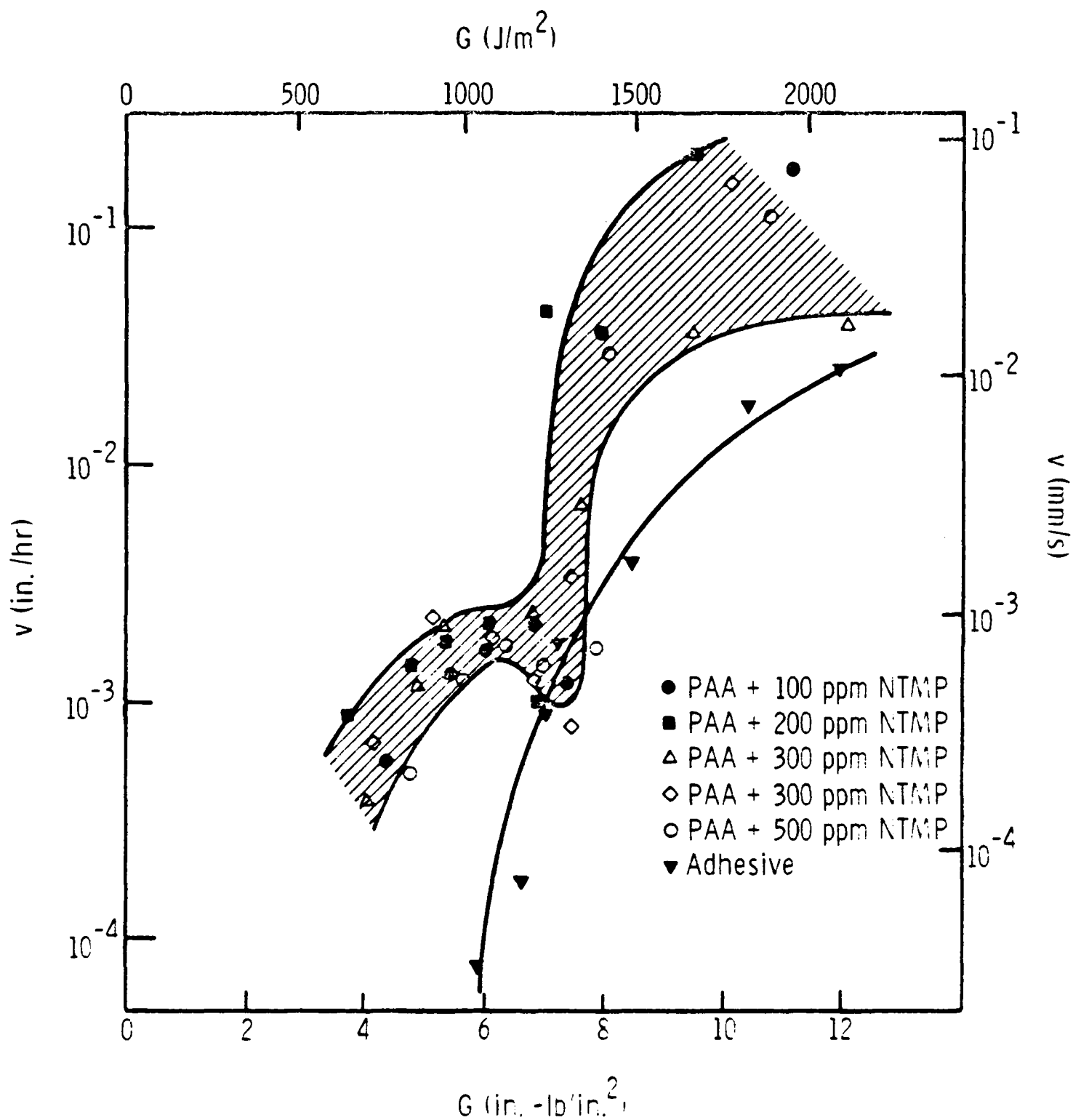
Figure 26. Wedge test results (crack velocity as a function of fracture energy) for NTMP-treated PAA adherends and FM 123-2 adhesive.[18]
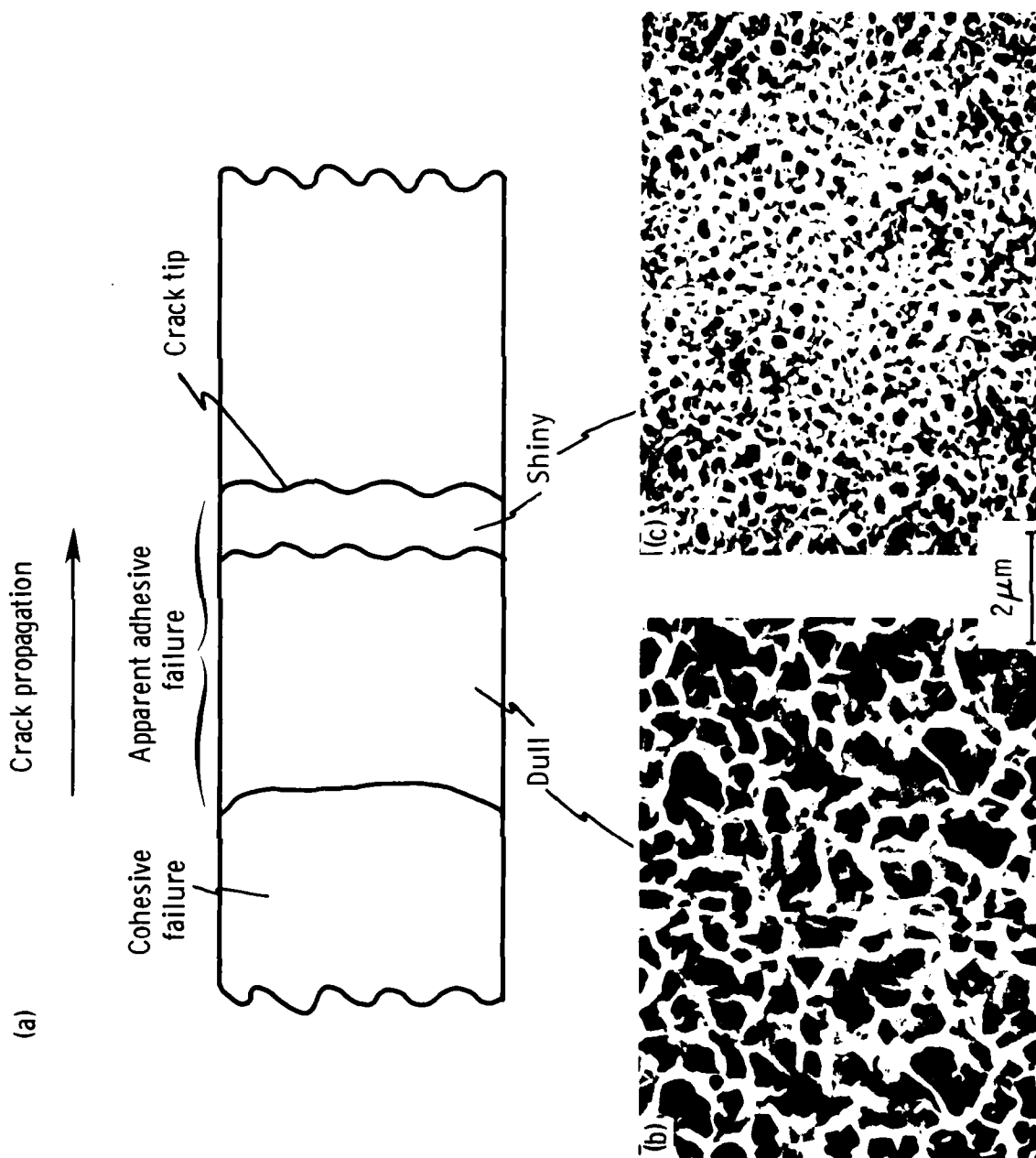
Figure 27. Fracture surface of wedge-test sample from untreated PAA adherends: a) schematic of surface, b) X-SEM stereo micrographs from dull area, and c) X-SEM stereo micrographs from shiny area.

epoxy resin between the oxide surface and the Dacron-reinforced adhesive, as shown in Fig. 27.

Conversion of oxide to hydroxide at the transition apparently occurs at such a low rate that it no longer is a precursor to crack propagation, and propagation through the adhesive becomes a more favorable mechanism of crack growth. The crack moves progressively away from the interface region until it is wholly within the adhesive layer (Fig. 28). The adhesive is deformed by the passage of the crack front until a deformation limit is exceeded, at which point it recoils to form the structure seen in Fig. 27c.

On PAA-treated adherends in the presence of the NTMP inhibitor, the transfer of the crack path away from the oxide/adhesive interface occurs at a shorter crack length, but at approximately the same exposure time. Figure 29 shows the fracture surface on the Al side of the adherend treated in a 200-ppm solution of NTMP. The crack has propagated through the adhesive, but is still quite close to the interface as indicated by the absence of reinforcing fibers. However, because moisture was still present, with the passage of sufficient time, estimated to be at least 100 hours, the oxide under the adhesive has transformed to boehmite, as shown by the cornflake structure below the thin adhesive layer. In fact, sufficient time has elapsed to allow bayerite crystallites to be solution-deposited on the adhesive surface.

The cracks in the adhesive layer are a direct result of the oxide-to-hydroxide conversion, which involves a lattice expansion and a more open morphology than that of the original amorphous oxide. This results in a 3-fold increase in the thickness of the layer under the adhesive[24], and a consequent strain which produces cracks in the adhesive. The dull and shiny fracture surfaces on PAA adherends were also analyzed by XPS and compared with results from an FPL-adherend fracture surface (Table X). The compositions of the dull PAA-fracture surface and the FPL failure surface were very similar and correspond to a boehmite-covered surface. The shiny surface, on the other hand, exhibited a very low Al concentration and a high C concentration,

Crack tip

Transfer of crack
to epoxy interface layer

Direction of crack propagation

Initial crack in adhesive

Re-initiation of crack
at Al metal/oxide interface

Al metal
Al oxide + epoxy
Epoxy
Epoxy + nylon
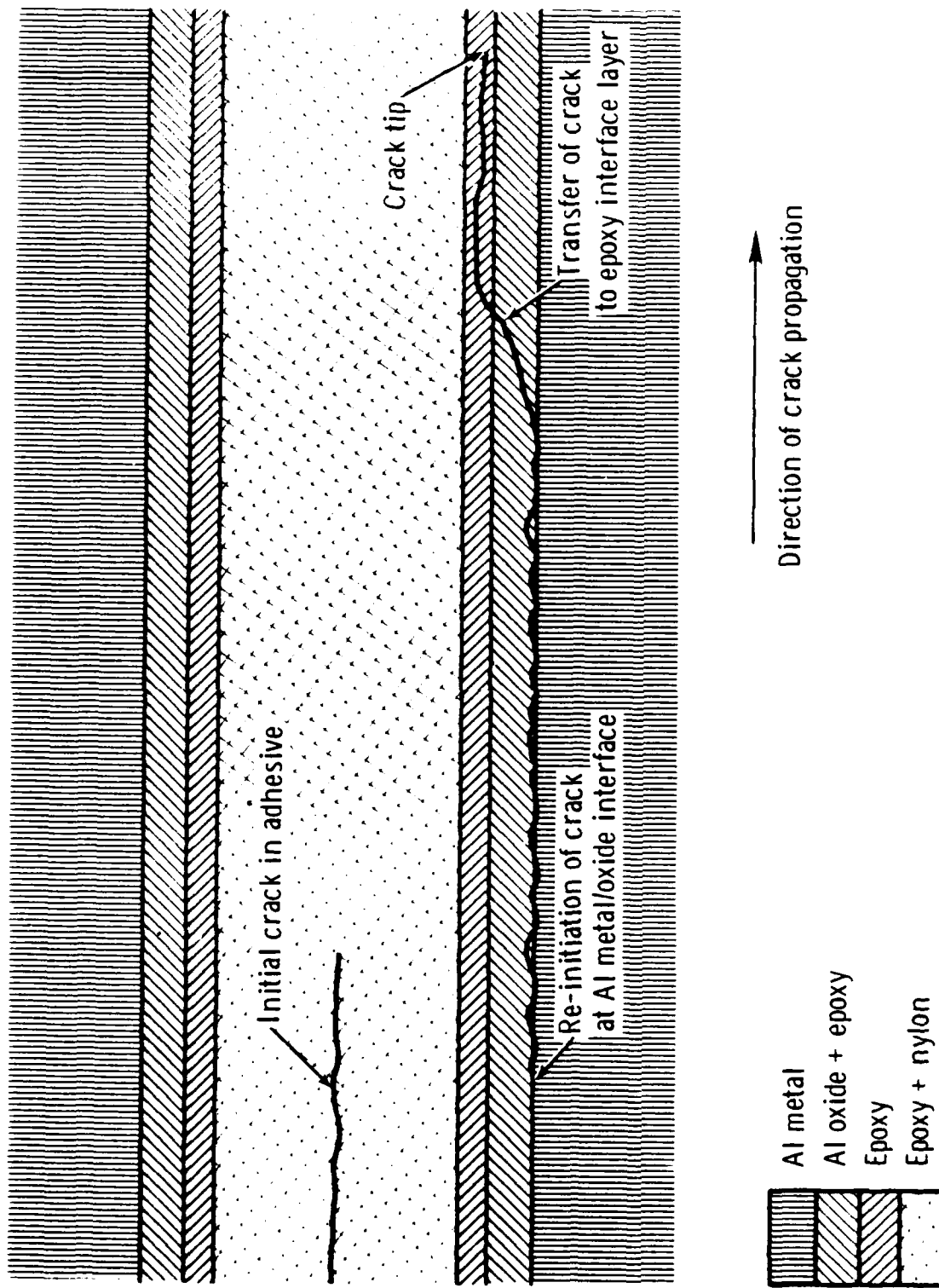
Figure 28. Schematic of crack path in wedge-test samples. (18)
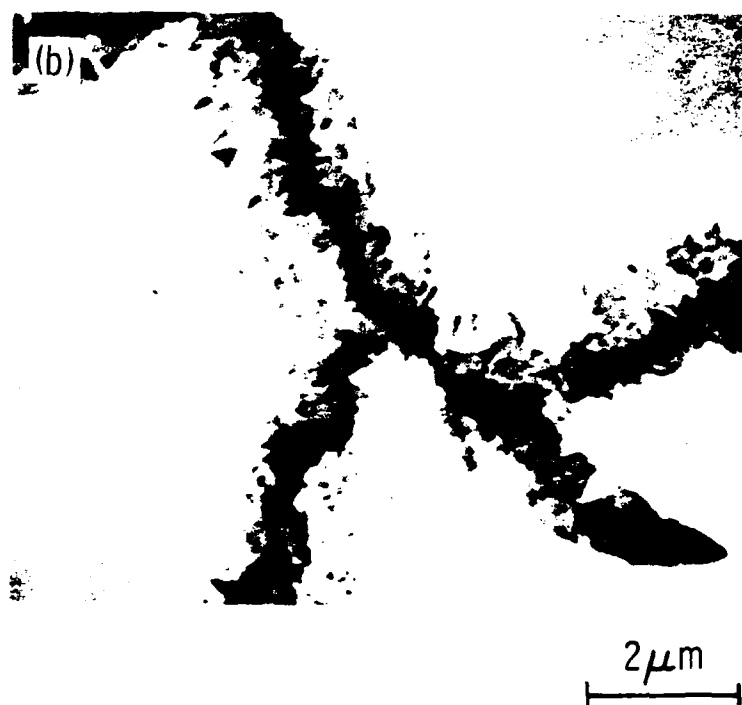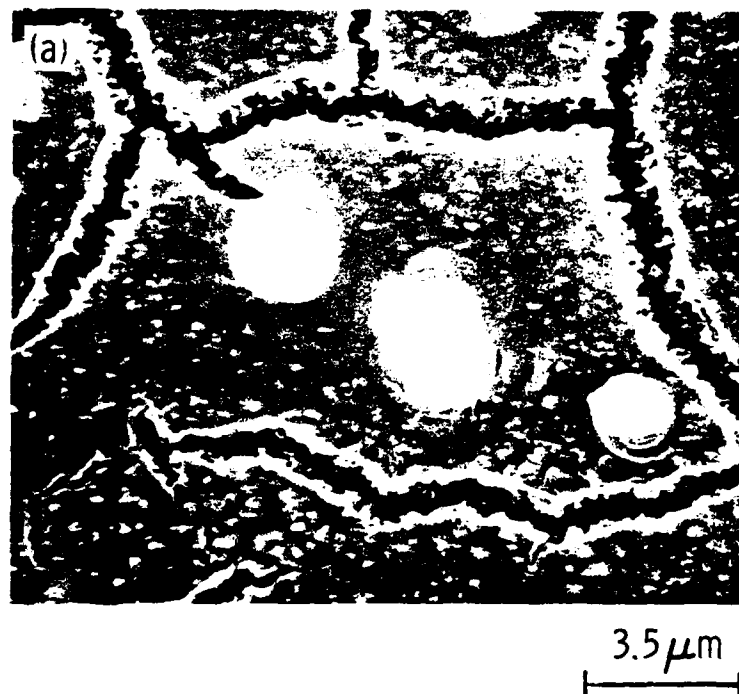
Figure 29. Micrographs of Al side of failed wedge-tested PAA samples treated in a 200-ppm solution of NTMP, b) higher magnification view of a).[18]

Table X

XPS Surface Composition of the Al Side of Wedge-
Tested PAA Adherends

Surface Description	Composition (at. %)		
(appearance)	Al	O	C
FPL	16	52	32
PAA (Dull)	22	46	32
PAA (Shiny)	3	18	79

confirming the X-SEM evidence that the shiny regions appear to be ruptured adhesive.

Furthermore, AES depth profiling shows the dull sample to be covered with an Al-hydroxide layer of $\sim$ 5,000-Å (Fig. 30). [Undulations in the aluminum and oxygen concentrations with depth may be due to density changes in the hydroxide layer or to artifacts from the measurement or sputtering processes on the extremely thick hydroxide layer.] In contrast, the shiny surface is shown to be an adhesive-reinforced oxide (resulting from interpenetration of the polymer into the oxide pores) $\sim$ 1,000-Å thick (Fig. 31) . In this case, hydration of the underlying oxide has not yet occurred.
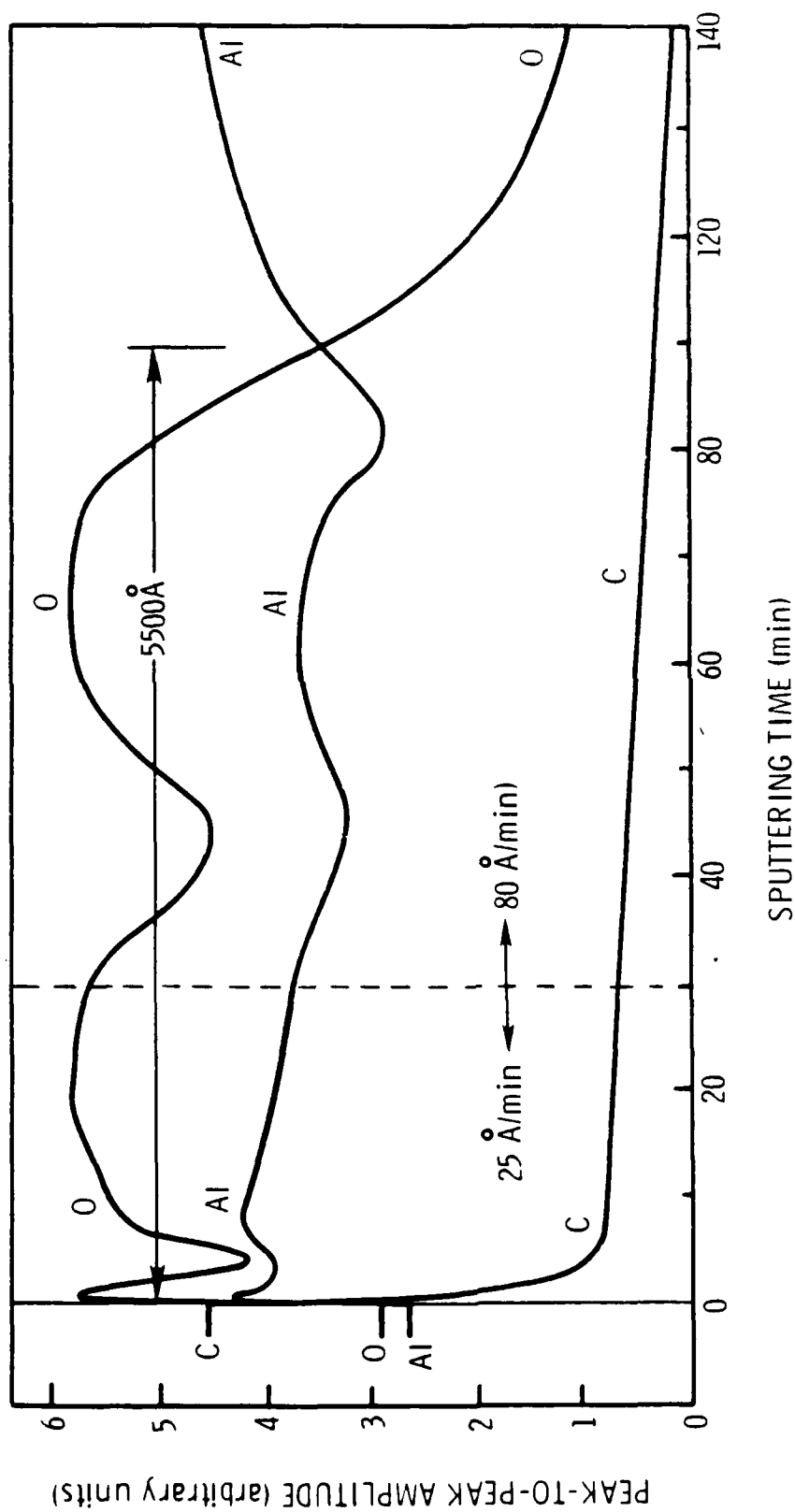
Figure 30. AES depth profile[18] "dull" region on Al side of PAA wedge-test failure surface.
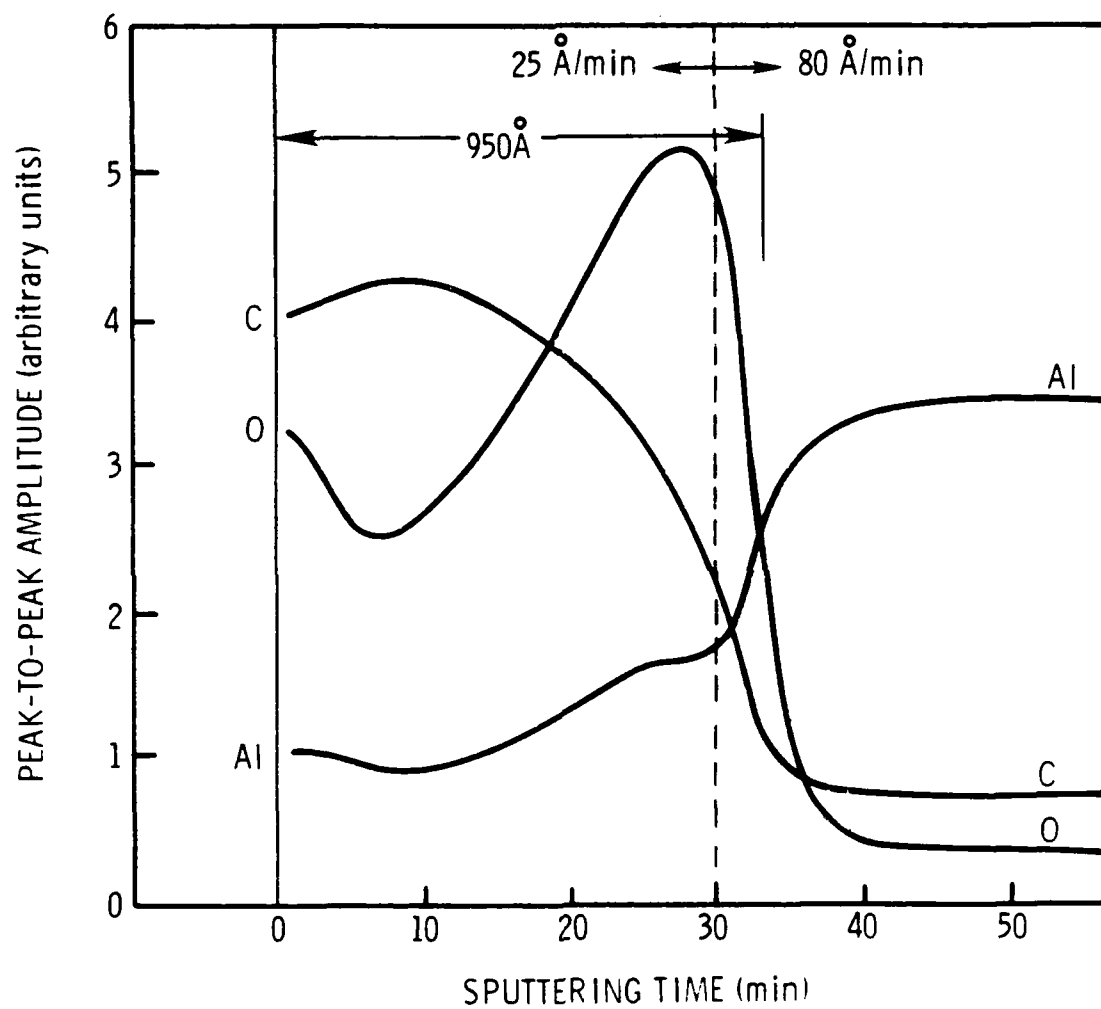
Figure 31. AES depth profile of "shiny" region on Al side of PAA wedge-test.[18]

IV. DISCUSSION

A. SURFACE CHEMISTRY

1. Inhibitor Adsorption

The adsorption onto FPL surfaces of each amino phosphonate inhibitor proceeds by the displacement of adsorbed water on the surface. For NTMP, this reaction continues at room temperature until most, if not all, the water is replaced by approximately one monolayer of chemisorbed inhibitor. However, AMP's water displacement process is less efficient, so that some water remains even at the highest AMP coverages achieved at room temperature. The presence of residual water is consistent with the lower phosphorus content on the surface at saturation. Our adsorption model suggests one phosphorus atom for every two water molecules removed from the surface (assuming that all the inhibitor's POH groups bond to the Al_2O_3). Since the AMP-treated surface has a significantly lower P/Al ratio, less water would have been displaced from the surface.

The adsorption data of NTMP on FPL (Fig. 5) show the adsorption isotherm to be concave downward, which is indicative of a two-step adsorption process. This is more clearly illustrated in Fig. 8, which shows the isotherm proceeding at first in the general direction of NTMP, but then heading away from the H_2O vertex. These results suggest that at very low solution concentrations, NTMP adsorbs with only one $PO_3^=$ group bonded to the surface. Consequently, the inhibitor coverage, as determined by the amount of P on the surface, increases faster than the water concentration on the surface decreases. At higher concentration, the NTMP competes more successfully with water for adsorption sites, and the other $PO_3^=$ groups of the molecule become bonded to the surface, displacing additional water without increasing the inhibitor coverage.

-60-

In contrast, a single-step process is expected for AMP, since it has only one phosphonic acid group per molecule. The SBD's shown in Figs. 7 and 8 support these ideas. Figure 8 clearly shows only a slight curvature in the surface composition evolutionary path for AMP on FPL, in contrast to the distinct two-step adsorption process for NTMP on FPL.

The adsorption of NTMP on PAA surfaces (Fig. 22) is quite different because little initial water is present to displace;[20] the resulting evolution of the surface composition suggests a simpler direct adsorption process. Nonetheless, the saturation coverage of phosphorus-containing groups is very similar between NTMP on PAA and NTMP on FPL. Although we cannot differentiate between NTMP adsorbing only on unoccupied active sites and NTMP displacing the phosphate incorporated onto the surface during anodization[20] in a competitive adsorption mechanism from these data alone, by comparing typical N concentrations on the NTMP/PAA and the NTMP/FPL surfaces ($\sim$ 1.5% and $\sim$ 2.5-3.0%, respectively), we note that the N ratio between treated PAA and FPL surfaces ($\sim$1:2) equals the corresponding ratio of additional P ($\sim$1:2, Fig. 21). These results allow us to eliminate the possibility of a significant displacement of the original phosphate and are, in fact, suggestive of a mechanism whereby NTMP adsorbs only an unoccupied active sites. Regardless of the details of the adsorption process, however, NTMP stabilizes the Al_2O_3 surface against hydration.

2.   Hydration

The behavior of the surface composition during the hydration of NTMP-treated FPL surfaces (Fig. 9) is very similar to the three-step process observed for PAA surface hydration.[20] First, a reversible physisorption of water occurs (as was discussed above). Next, the surface hydrates to boehmite forming the cornflake morphology. Finally, there is further hydration as bayerite crystallites grow on top of the boehmite. It is during the second stage that adhesive bonds fail; consequently, an understanding of events occurring during this period should be beneficial in deducing the important characteristics of inhibitors and ultimately in improving bond durability. Such an understanding is obtainable from our results: The linear paths of the

surface composition in the SBD of Fig. 9, together with the absence of any subsurface phosphorus in the hydration product, indicates that hydration occurs only as the NTMP-Al complex slowly dissolves from the surface. This complex apparently forms an ultra-thin protective coating by adsorbing onto active sites. However, as this molecular film is removed, the surface exhibits the low resistance to hydration of the original FPL oxide.

B. MECHANICAL PROPERTIES

1. Initial Dry Strength

Use of epoxy adhesives in T-peel and double-lap-shear tests of treated and untreated structures demonstrates that optimum initial dry strength is exhibited by the control specimens since failure was cohesive in the adhesive. Consequently, no improvement was expected or observed for inhibitor-treated adherends. The observation that the treated specimens exhibit dry performance equal to that of the controls indicates that the interfacial strength between the oxide and adhesive remains stronger than the cohesive strength of the adhesive.

The small degradation of T-peel strengths of primed, treated structures bonded with the nitrile phenolic adhesive suggests that these inhibitors may not be compatible with all types of adhesives. However, even in these cases, failure occurred within the polymer system, possibly at the primer-adhesive interface. The inhibitors, then, do not weaken the primer-aluminum oxide interface below the cohesive strength of the polymer system, but do apparently reduce the cohesive strength itself, possibly by inhibiting the cure of the polymer, thereby weakening the bond. Clearly the compatibility of an inhibitor with a non-epoxy-based adhesive system must be determined before use.

2. Bond Durability

The wedge test results for FPL adherends treated in NTMP solutions at room temperature indicate that such treatment results in marked improvements in environmental durability, as measured by the final crack length after exposure to a humid environment. The observation of similar Al concentrations on both sides of the failure surface (Tables IX and X) of the FPL adherends confirmed previous observations[6] that the locus of failure was through a hydrated oxide layer. In the presence of moisture, the original Al oxide is converted to Al hydroxide. The formation of boehmite from the initial oxide involves a lattice expansion and the cornflake morphology characteristically adopted by the boehmite is considerably less dense than that of the original amorphous oxide. This oxide-to-hydroxide conversion disrupts the mechanical interlocking between the oxide and the adhesive and creates stresses that promote crack propagation along the weak hydroxide-metal interface.

Maximum improvements in bond durability are associated with room-temperature saturation surface coverage (approximately one monolayer). Higher coverage, such as that obtained by NTMP treatment at 80°C, did not further improve the bond durability. In fact, XPS results from the failure surfaces of 80°C-treated FPL bondments showed that P was present on both the aluminum and adhesive sides, and the Al concentration on the adhesive side was quite low (Table IX). These results suggest that crack propagation occurred at least partially through the NTMP multilayer at the oxide-adhesive interface.

The improvements in bond durability that accompany NTMP surface pre-treatments result from stabilization of the surface against hydration, as shown by the incubation-time measurements of Table III. In fact, in some cases, the hydration rate of NTMP-treated specimens is slowed sufficiently so that it is no longer the limiting factor in bond durability. Instead, at least at the latter stages of crack growth, failure occurs along the inhibitor-adhesive interface and only after subsequent exposure does the oxide surface hydrate (Fig. 19).

Failure in these cases (and in the experiment involving NTMP treatment at elevated temperatures) may be caused by slow moisture-induced changes in the adhesive (similar to those seen by Albrecht and Mecklenburg[26]), which allow the adhesive to relax and withdraw from the nooks and crannies of the FPL oxide. Such a phenomenon would only be seen with configurations such as those used in wedge tests where water is in contact with the adhesive at the crack tip for extended periods of time. Additionally, this relaxation of the adhesive could be observed only in conjunction with a very stable oxide.

The improvements in bond durability conferred by the inhibitor treatment can be assessed quantitatively with the fracture energy analysis of the wedge-test data. The values of G_I in Table VIII are specific to the test conditions used and the assumptions made in their calculation. However, they do indicate that NTMP treatment results in a 4-fold average increase in G_I.

In all cases, insertion of the wedge-test assemblies into the warm humid environment resulted in the initiation of a crack at or near the oxide/adhesive interface. This crack initiation has also been observed by other investigators[27] and is apparently due to hydration of the oxide and the associated breakdown of interface integrity. If moisture is excluded from the interface, interfacial failure does not occur.

The bond durability of PAA-treated adherends is also increased by treatment in NTMP solutions at room temperature. Again, additional adsorbed NTMP (from high-temperature solutions) did not further increase wedge-test performance; in fact, in the one set of experiments performed, performance of the higher NTMP coverage panels was inferior to that of panels treated at room temperatures. The reason for this decrease is not known; crack propagation at the latter stages is not hydration controlled even in the untreated specimens, but may be influenced by coupling of the oxide to the adhesive through the inhibitor (coupling will be discussed in more detail in the comparison of different inhibitors, p. 67) An NTMP multilayer would be limited by weak

intermolecular bonding and would not be as efficient a coupling agent as an NTMP monolayer.

When the wedge-test data are analyzed using the fracture mechanics approach, it is clear that adherend behavior is strongly dependent on surface treatment prior to bonding. This is illustrated in Figs. 12, 13, 25 and 26, which include data for adherend surfaces treated with FPL, FPL + NTMP, PAA, PAA + NTMP, and the adhesive bonded to PAA adherends. Insertion of the wedge-test assemblies into the warm humid environment initiated a crack at or near the adhesive/oxide interface. As previously discussed, there is an abrupt transition of FPL adherends from cohesive to adhesive failure during the first hour of exposure to the humid environment. This transition is less abrupt for the PAA adherends and, on PAA treated with saturation surface coverages of NTMP, there is effectively an "incubation period" before interfacial failure is observed.

The initiation and propagation of the interface crack is apparently due to direct hydration of the oxide or weakening of the adhesive-inhibitor interface and the associated breakdown of interface integrity. If cohesive failure is forced by using a corrosion inhibiting primer prior to bonding, then optimum bond durability for our test system for PAA adherends can be achieved because only the adhesive behavior under stress in a warm, humid environment is involved.

Once interfacial cracking has begun on FPL adherends, the initial crack velocity is maintained to very low G values, indicating that the mechanism of crack growth is independent of the stress (Figs. 12 and 23). Indeed, the conversion of oxide to hydroxide is such a stress-independent mechanism.

The behavior of PAA adherends is quite different. At G levels that are still relatively high, the crack velocity falls two orders of magnitude below its initial value. Examination of these fracture surfaces by X-SEM revealed that the locus of failure initially is through the oxide, but in latter stages, it goes through the adhesive near the oxide-adhesive interface.

On PAA adherends treated in NTMP solutions this transfer into the adhesive layer near the interface occurs at a small crack extension, but at approximately the same exposure time as untreated PAA adherends. The discontinuity in the behavior of these adherends evident in Figs. 25 and 26 is probably a reflection of this change in the locus of failure. The behavior at the higher G levels is evidence of failure of the adherend through oxide hydration, whereas at the lower G levels it is characteristic of the adhesive near the interface. The v-G curve for the inhibited PAA adherends approaches that of the adhesive. The crack velocity does not follow the adhesive curve because the locus of failure is in the near interface region where the adhesive is not reinforced.

We speculate that the transition between crack propagation in the oxide and in the adhesive may involve the slow moisture-induced relaxation of the adhesive mentioned earlier. Unlike the situation with FPL adherends, the adhesive is not able to disengage from the more extensive mechanical interlocking provided by PAA oxide. However, the interlocking could be weakened, thereby allowing the crack to move upward in the oxide to the unreinforced adhesive. Regardless of the mechanism by which the crack transfers from the oxide to the adhesive, the unreinforced adhesive is not as durable as the reinforced adhesive. The failure of the crack to transfer to the near interfacial region in tests giving totally cohesive failure (primed PAA specimens and samples not exposed to high humidity) suggests that an activation energy for crack transfer or crack re-initiation is necessary. Otherwise the crack would not have remained within the Dacron-reinforced region.

It is interesting to note that despite the dramatic improvement that treatment with NTMP (or the other inhibitors) provides in wedge-test results, no improvement was seen in the double-lap-shear experiments using FPL adherends. We attribute this to the severity of the wedge test conditions (water present at a crack tip under stress) which promote surface hydration. In contrast, in a double-lap-shear configuration, water must diffuse through

the adhesive or along the adhesive-oxide interface in order to attack the oxide. Considerably longer exposure times to moisture would be expected to induce interfacial failure. This is, in fact, the case; crack propagation in our exposed double-lap-shear specimens was within the adhesive. In the time-frame chosen (7-day exposure), interface stability is not the weakest link of the system and the hydration inhibitors would not be expected to improve performance.

3. Inhibitor Evaluation

Several different inhibitors beside NTMP have also been investigated, but in less detail. The first of these, PA, is of interest because the PA-adsorbed FPL surface is analogous to the PAA surface in that both exhibit similar P/Al ratios and hydration resistance. However, their wedge-test performances are markedly different: treatment in PA solutions provides no improvement in bond durability over that of the FPL control. Results of XPS failure analysis of a 66-ppm PA specimen and, to a lesser extent, a 33-ppm specimen (Table IX) indicate failure along the oxide-adhesive interface, probably prior to hydration since P was detected on the metal side of the 66 ppm sample. Apparently PA weakens this interface, relative to NTMP-treated interfaces, either by forming inhibitor-adhesive bonds that are not resistant to attack by moisture or by passivating the adherend surface and forming no chemical bonds with the adhesive. In both cases, the interface provides an easy path for crack propagation following possible moisture-induced relaxation of the adhesive. We will return to the idea of chemical bonding between the adhesive and the inhibitor in the discussion of other inhibitors.

Given that PA-treated FPL samples provide poor bond durability despite a similar surface chemistry (as measured by XPS) to PAA samples, what accounts for the superior performance of PAA specimens during wedge tests? We attribute this to the significantly thicker and more evolved oxide formed by the PAA process whereby the physical interlocking is more extensive and efficient. Consequently, bond performance is less dependent on chemical

coupling of the oxide and the adhesive. Any degradation between a PA-like film and the adhesive should have less effect on the bond durability of PAA adherends because the substantial interlocking of oxide and adhesive will retard crack propagation (provided stability of the oxide is maintained).

Many of the remaining inhibitors, such as MP and AMP, can be discussed in pairs. Despite their good initial bond strengths (Table IV), MP-treated adherends performed very poorly in wedge tests, i.e., their bond durability was actually below that of the untreated FPL control specimens. Crack propagation occurred interfacially between the oxide and the adhesive. The reasons for this very poor performance are not completely understood. The same factors governing the durability of PA-treated FPL samples may be more important here, causing reduced wetting of the oxide by the adhesive and consequently less mechanical interlocking. Regardless of the explanation for the MP results, those of AMP show that the addition of the amino group to MP makes a dramatic difference in the performance of the respective bonds. This amino group is capable of reacting with the epoxy adhesive, thus strengthening the inhibitor-adhesive interface. Concurrently, by making a less soluble complex, the inhibitor probably increases the hydration resistance of the oxide, even though the water that remains on the surface following saturation coverage of AMP (Figs. 7 and 8) can act as initiation sites for hydration. These initiation sites prevent the hydration resistance from becoming as high as that of NTMP-treated oxides.

The next set, the two (Bu)NBMP compounds and the (n Bu)ANBMP, each exhibit improved durability, with (n Bu)NBMP and (n Bu)ANBMP treatments giving wedge test performance comparable to that of NTMP treatment. Failure occurs as the oxide hydrates, leading to crack propagation within the hydroxide or along the weak hydroxide-metal interface with subsequent hydration of the exposed metal surface.

We attribute the improved performance of the (n Bu)NBMP and (n Bu)ANBMP samples over those treated with (t Bu)NBMP to a molecular mechanical

interlocking or good dispersion of the n-butyl tail in the polymeric adhesive as contrasted with the inert, compact t-butyl cluster. This mechanical and, in the case of (n Bu)ANBMP, chemical coupling would make the interface less vulnerable to aqueous attack and improve bond durability. However, it cannot fully compensate for the reduced number of inhibitor-oxide bonds formed by the (Bu)NBMP compounds compared with those formed by NTMP. As a result, treatment with (n Bu)NBMP or (n Bu)ANBMP fails to provide superior performance to that of NTMP-treated adherends.

Each of the remaining inhibitors has four methylene phosphonic acid groups to increase bonding to the aluminum oxide. The first of these, EDTMP, is essentially two NTMP molecules joined together. Treatment with EDTMP or with NTMP provides very similar performance, with failure occurring, at least partially, interfacially. Such results suggest that increasing the inhibitor-oxide bonding over that of NTMP does not lead to improved bond durability.

The final set of inhibitors, 2ϕ and 2pA, form another inert/reactive pair, with the 2pA containing an amine group to react with the epoxy adhesive. Although poorer than expected durability was noted for adherends treated in 2pA, performance equivalent to the best provided by any inhibitor treatment was seen for panels immersed in 2ϕ. We attribute the 2pA results to residual impurities mixed with the inhibitor following synthesis. Purer material would presumably have provided durability equal to or better than that of 2ϕ.

4. Inhibitor Properties for Improving Bond Durability

Based on the surface chemistry measurements and the mechanical test results just presented, we have identified five criteria or properties important for inhibitors to improve bond durability of aluminum structures: 1) occupation of all active sites on the Al_2O_3 surface, 2) formation of strong inhibitor-aluminum oxide bonds, 3) insolubility of the resulting inhibitor-

aluminum complex in aqueous solutions, 4) compatibility with the adhesive/primer, and 5) coupling to the adhesive/primer.

The first three were derived from the models of adsorption and hydration. Strong interactions between the inhibitor and the adherend surface are needed so that the inhibitor in a dilute solution can successfully compete with water for adsorption sites and effectively passivate all the surface sites subject to initiation of hydration. Furthermore, once the aluminum-inhibitor complex is formed, it must remain on the surface to protect the underlying oxide and not go into solution.

The fourth criteria--compatibility--was suggested by T-peel experiments in which inhibited specimens exhibited low initial strength when bonded with a nitrile phenolic adhesive. The poor durability of the MP-treated wedge test panels are also being explained in terms of poor compatibility under moist conditions.

Finally, the importance of coupling to the adhesive was noted in many of the inhibitor comparisons using wedge-test data. The coupling can be chemical, as illustrated by the improved durability of AMP-treated samples over that of MP-treated specimens; it can be mechanical on a molecular scale, as demonstrated by the results of the two (Bu)NBMP compounds; or it can be electron donor/acceptor bonding as indicated by the relative performance of PA- and NTMP-treated FPL panels. In the last case, the lone pair of electrons on the NTMP nitrogen apparently interact with the polymeric adhesive to provide superior bond durability for NTMP-treated adherends compared to that of PA-treated structures even though each compound is effective in inhibiting hydration.

Although presented as such, these criteria are not independent. For example, an inhibitor that occupies all active sites on the surface would undoubtedly be strongly bonded to the surface. Similarly, an inhibitor that couples to an adhesive would also be compatible with it and would form a complex less likely to be attacked by water. Once the oxide surface is

stabilized with respect to hydration, coupling to the adhesive can also become important in preventing or slowing moisture-induced changes in the adhesive from disengaging from the microroughness of the oxide. This is especially important for the less rough FPL oxide, as demonstrated by the PA and NTMP results, but was also seen in the inhibited and untreated PAA oxides. In fact, for the NTMP/FPL case, the hydration was slowed sufficiently for the withdrawal of the adhesive from the oxide to be the limiting factor in bond durability.

V. SUMMARY

We have investigated the use of hydration inhibitors, such as nitrilotris methylene phosphonic acid (NTMP), to improve the durability of adhesively bonded aluminum structures placed in a moist environment. We showed that: 1) pretreatment of FPL adherends in an inhibitor solution increases bond durability dramatically, so that, in some cases, hydration of the adherend is no longer the limiting step in crack propagation; 2) pretreatment of PAA adherends further improves durability so that the transition to failure in the adhesive occurs at a shorter crack length; 3) such pretreatments involve no change in the initial strength for bonds using epoxy adhesives; 4) adsorption of NTMP onto an FPL surface involves the displacement of water initially present with the formation of P-O-Al bonds for a saturation coverage of approximately one monolayer; 5) adsorption of NTMP onto a PAA surface results in occupation of residual active sites on a surface with little initial water; 6) hydration of an inhibited FPL surface proceeds in three steps: i) a reversible physisorption of water, ii) a slow dissolution of the inhibitor-aluminum complex followed by rapid hydration of the freshly exposed amorphous aluminum oxide to boehmite, and iii) a further hydration of the boehmite to bayerite; and, finally, 7) several criteria are important for inhibitors designed to improve bond durability: i) displacement of water and occupation of all active sites on the Al_2O_3 surface, ii) formation of strong inhibitor surface bonds, iii) insolubility of the resulting inhibitor-aluminum complex in aqueous solutions, iv) compatibility with the adhesive or primer, and v) coupling of the inhibitor to the adhesive.

VI. REFERENCES

1. H.W. Eichner and W.E. Schowalter, Forest Products Laboratory, Madison, WI, Report No. 1813, 1950.

2. G.S. Kabayaski and D.J. Donnelly, Boeing Corporation, Seattle, WA, Report No. D6-41517, February 1974.

3. J.D. Venables, D.K. McNamara, J.M. Chen, and T.S. Sun, Appl. Surf. Sci. 3, 88 (1979).

4. J.D. Venables, J. Mater. Sci. 19, 2431 (1984).

5. D.J. Packham, in Adhesion Aspects of Polymeric Coatings, ed. K.L. Mittal, Plenum, New York, 1983, p. 13, and the references therein.

6. J.D. Venables, D.K. McNamara, J.M. Chen, B.M. Ditchek, T.I. Morgenthaler, and T.S. Sun, in Proc. 12th Natl. SAMPE Tech. Conf., Seattle, WA, 1980, p. 909.

7. D.A. Hardwick, J.S. Ahearn, and J.D. Venables, MML TR 82-23c, End-of-Second-Year Report under ONR Contract N00014-80-C-0718, Martin Marietta Laboratories, Baltimore, MD, November 1982.

8. J.S. Ahearn, G.D. Davis, A.I. Desai, and J.D. Venables, MML TR 81-46c, End-of-First-Year Report under ONR Contract N00014-80-C-0718, Martin Marietta Laboratories, Baltimore, MD, October 1981.

9. G.D. Davis, J.S. Ahearn, and J.D. Venables, MML TR 83-34c, End-of-Third-Year Report under ONR Contract N00014-80-C-0718, Martin Marietta Laboratories, Baltimore, MD, November 1983.

10. G.D. Davis, J.S. Ahearn, L.J. Matienzo, and J.D. Venables, MML TR 84-54c, End-of-Fourth-Year Report under ONR Contract N00014-80-C-0718, Martin Marietta Laboratories, Baltimore, MD, November 1984.

11. J.S. Ahearn, G.D. Davis, T.S. Sun, and J.D. Venables, in Adhesion Aspects of Polymeric Coatings, ed., K.L. Mittal, Plenum, New York, 1983, p. 281.

12. G.D. Davis, J.S. Ahearn, and J.D. Venables, in Proc. 15th Natl. SAMPE Tech. Conf., Cincinnati, OH, 1983, p. 202.

13. G.D. Davis and J.D. Venables, in Durability of Adhesive Bonds, ed. A.J. Kinloch, Applied Science, Essex, 1983, p. 43.

14. D.A. Hardwick, J.S. Ahearn, and J.D. Venables, J. Mater. Sci. 19, 223 (1984).

15. G.D. Davis, J.S. Ahearn, and J.D. Venables, J. Vac. Sci. Technol. A 2, 763 (1984).

16. G.D. Davis, J.S. Ahearn, and J.D. Venables, in Proc. Int. Adhesion Conf. 1984, Nottingham, England, 1984, p. 12al.

17. G.D. Davis, J.S. Ahearn, L.J. Matienzo, and J.D. Venables, Martin Marietta Labs, J. Mater. Sci. (in press).

18. D.A. Hardwick, J.S. Ahearn, A. Desai, and J.D. Venables, accepted by J. Mater. Sci.

19. J.D. Venables, M.E. Tadros, and B.M. Ditchek, US Patent 4,308,079.

20. G.D. Davis, T.S. Sun, J.S. Ahearn, and J.D. Venables, J. Mater. Sci. 17, 1807 (1982).

21. G.D. Davis, S.P. Buchner, W.A. Beck, and N.E. Byer, Appl. Surf. Sci. 15, 238 (1983).

22. D. Broek, Elementary Engineering Fracture Mechanics, Sythoff and Noordhoff, The Netherlands, 1978, p. 154.

23. M.H. Stone and T. Peet, Royal Aircraft Establishment, Tech. Memo MAT 349, July 1980.

24. T.S. Sun, J.M. Chen, J.D. Venables, and R. Hopping, Appl. Surf. Sci. 1, 202 (1978).

25. W. Vedder and D.A. Vermilyea, Trans. Faraday Soc. 65, 561 (1960).

26. P.A. Albrecht and M.M. Mecklenburg, University of Maryland - College Park (personal communication).

27. R.L. Patrick, J.A. Brown, L.S. Verhoeven, E.D. Ripling, and S. Mostovoy, J. Adhes. 1, 136 (1969).

VII. <u>ACKNOWLEDGEMENTS</u>

Technical Reports
Under ONR Contract N00014-80-C-0718

1. J.S. Ahearn, G.D. Davis, A.I. Desai, and J.D. Venables, MML TR 81-46c, End-of-First-Year Report, "Mechanical Properties of Adhesively Bonded Aluminum Structures Protected with Hydration Inhibitors," Martin Marietta Laboratories, Baltimore, MD, October 1981.

2. D.A. Hardwick, J.S. Ahearn, and J.D. Venables, MML TR 82-23c, End-of-Second-Year Report, "Mechanical Properties of Adhesively Bonded Aluminum Structures Protected with Hydration Inhibitors," Martin Marietta Laboratories, Baltimore, MD, November 1982.

3. D.A. Hardwick, J.S. Ahearn, and J.D. Venables, MML TR 83-5, "Environmental Durability of Aluminum Adhesive Joints Protected with Hydration Inhibitors," Martin Marietta Laboratories, Baltimore, MD, March 1983.

4. G.D. Davis, J.S. Ahearn, and J.D. Venables, MML TR 83-34c, End-of-Third-Year Report, "Mechanical Properties of Adhesively Bonded Aluminum Structures Protected with Hydration Inhibitors," Martin Marietta Laboratories, Baltimore, MD November 1983.

5. G.D. Davis, J.S. Ahearn, L.J. Matienzo, and J.D. Venables, MML TR 84-54c, End-of-Fourth-Year Report, "Mechanical Properties of Adhesively Bonded Aluminum Structures Protected with Hydration Inhibitors," Martin Marietta Laboratories, Baltimore, MD, November 1984.

List of Presentations
under ONR contract N00014-80-C-0718

1. "Correlation of Surface Chemistry and Mechanical Properties of Aluminum Substrates Bonded to Polymer Coatings: I. Surface Chemistry," T.S. Sun, G.D. Davis, B.M. Ditcheck, J.S. Ahearn, and J.D. Venables, Electrochemical Society Meeting, Symposium on Adhesion Aspects of Polymeric Coatings, Minneapolis, MN, 10-15 May 1981.

2. Correlation of Surface Chemistry and Mechanical Properties of Aluminum Substrates Bonded to Polymer Coatings: II. Mechanical Properties," J.S. Ahearn, T.S. Sun, D.K. McNamara, B.M. Ditchek, and J.D. Venables, Electro-chemical Society Meeting, Symposium on Adhesion Aspects of Polymeric Coatings, Minneapolis, MN, 10-15 May 1981.

3. "Adhesive Bonding of Aluminum," J.S. Ahearn, University of Bath, Bath, England, 23 October 1981 (INVITED).

4. "Adhesive Bonding of Aluminum," J.S. Ahearn, City University of London, London, England, 20 November 1981 (INVITED).

5. "Adhesive Bonding of Aluminum," J.S. Ahearn, New University of Ulster, Northern Ireland, 27 November 1981 (INVITED).

6. "Adhesive Bonding of Aluminum," J.S. Ahearn, University of Warwick, Coventry, England, 4 December 1981 (INVITED).

7. "Surface Science Related Research at Martin Marietta Laboratories," J.M. Chen, Naval Surface Weapons Center, White Oak, MD, 24 April 1981 (INVITED).

8. "Science of Adhesion," J.D. Venables, NASA Lewis Research Center, Cleveland, OH, 7 April 1981 (INVITED).

9. "Durability of Adhesive Bonds to Al and Ti," J.D. Venables, DoD Workshop on Adhesive Bonding, Dayton, OH, 23 April 1981 (INVITED).

10. "Science of Adhesion," J.D. Venables, Lehigh University, Bethlehem, PA, 28 April 1981 (INVITED).

11. "Science of Adhesion," J.D. Venables, Old Dominion University, Norfolk, VA, 30 April 1981 (INVITED).

12. "Surface Science - Introduction and Selected Applications," G.D. Davis, Old Dominion University, Norfolk, VA, 18 February 1982 (INVITED).

13. "Adhesion and Durability of Metal/Polymer Bonds," J.D. Venables, Adhesion Society Meeting, Mobile, AL, 22 February 1982 (INVITED).

14. "Adhesion and Durability of Metal/Polymer Bonds," J.D. Venables, Piedmont Section of ASM, Winston Salem, NC, 4 March 1982.

15. "Use of Surface Behavior Diagrams to Study Adhesive Bond Durability" G.D. Davis and J.D. Venables, 56th Colloid and Surface Science Symposium, Blacksburg, VA, 14 June 1982.

16. "Adhesion and Durability of Metal/Polymer Bonds," J.D. Venables, Int'l Symposium on Adhesive Joints, Amer. Chem. Soc., Kansas City, MO, 12-16 September 1982 (INVITED).

17. "Science of Adhesive Bonding," J.D. Venables, Naval Surface Weapons Center, White Oak, MD, 10 November 1982 (INVITED).

18. "Protective Coatings," J.D. Venables, ARO Workshop, Charleston, SC, 15 December 1982 (INVITED).

19. "Use of Surface Behavior Diagrams to Study Surface Reactions," G.D. Davis, Northeast ESCA User's Group Meeting XXIII, Silver Spring, MD, 10 December 1982.

20. "New Approaches for Studying Moisture Sensitivity of Adhesive Bonds," G.D. Davis, NAVAIR Corrosion Technology Review, Warminster, PA, 15 March, 1983 (INVITED).

21. "Surface Behavior Diagrams to Study Chemical Reactions on Surfaces," G.D. Davis, University of Maryland - Baltimore County, Baltimore, MD, 4 April 1983 (INVITED).

22. "Surface Behavior Diagram Study of the Adhesive Bonding of Aluminum," G.D. Davis, Rensselaer Polytechnic Institute, Troy, NY, 11 April 1983 (INVITED).

23. "Surface Behavior Diagram Study of the Adhesive Bonding of Aluminum," G.D. Davis, University of Wisconsin, Madison, WI, 28 April 1983 (INVITED).

24. "Applications of Tunneling Spectroscopy to the Study of Adhesion," H.W. White, 3rd Intl. Symp. on Adhesion, Washington State University, Pullman, WA, 26-29 Sept. 1983.

25. "Fundamental Investigation of Mechanisms Coupling Tunneling Electrons to Vibrating Molecules in IETS," C.D. Crowder, G.P. Alldredge, and H.W. White, 9th Intl. Vacuum Congress and 5th Intl. Conf. on Solid Surfaces, Madrid, Spain, 26 September-1 October 1983.

26. "Adhesion and Durability of Metal/Polymer Bonds," J.D. Venables, ASM Meeting, Waterloo, IA, 4 October 1983.

27. "Adhesion and Durability of Metal/Polymer Bonds," J.D. Venables, Virginia Polytechnic Institute, Blacksburg, VA, 31 October 1983 (INVITED).

28. "Adhesive Bonding of Al and Ti," M. Natan, Department of Defense, Aeronautical Research Laboratories, Melbourne, Australia, 19 October 1983.

29. "Adhesive Bonding of Al and Ti," M. Natan, Hawker De Havilland, Sydney, Australia, 4 November 1983.

30. "Hydration of Aluminum Adherends as Studied by Surface Behavior Diagrams," G.D. Davis, J.S. Ahearn, and J.D. Venables, 15th Natl. SAMPE Techn. Conf., Cincinnati, OH, 5 October 1983 (INVITED).

31. "Use of Surface Behavior Diagrams to Study Hydration/Corrosion of Aluminum and Steel Surfaces," G.D. Davis, J.S. Ahearn, and J.D. Venables, 30th Natl. Symp. American Vacuum Society, Boston, MA, 1 November 1983.

32. "Hydration Inhibitor Properties for Improved Durability of Aluminum Adhesive Bonds," G.D. Davis, J.S. Ahearn, and J.D. Venables, ARO Work Group Meeting on Principles and Applications of Electrochemistry, Charleston, SC, 14 December 1983 (INVITED).

33. "Applications of Tunneling and Electrostatic Potential Calculations to the Study of Inhibition," H.W. White, ARO Work Group Meeting on Principles and Applications of Electrochemistry, Charleston, SC, 14 December 1983 (INVITED).

34. "Science of Adhesion," J.D. Venables, ASTM D14 Committee on Adhesion Denver, CO, March 1984.

35. "Science of Adhesion," J.D. Venables, National Academy of Science Workshop on Adhesive Bonding, Washington, DC, May 1984 (INVITED).

36. "Role of Materials Science in High Technology Manufacturing," J.D. Venables, Sagamore Conf. on Materials Characterization, Lake Lucerne, NY, August 1984 (INVITED).

37. "Surface Behavior Diagrams: XPS Characterization of Metal Oxides," G.D. Davis, Gordon Reseach Conf. on Adhesion Science, New Hampton, NH, 21 August 1984 (INVITED).

38. "Study of Adhesive Bond Durability Using XPS Surface Behavior Diagrams," G.D. Davis, University of Warwick, Coventry, England, 10 September 1984 (INVITED).

39. "Hydration Inhibitor Properties for Improved Durability of Aluminum Adhesive Bonds," G.D. Davis, J.S. Ahearn, and J.D. Venables, Intl. Adhesion Conf. 1984, Nottingham, England, 12 September 1984 (INVITED).

40. "Surface Behavior Diagrams Applied to Adhesive Bonding," G.D. Davis, 2nd Symp. Welding, Bonding, and Fastening, Hampton, VA, 25 October 1984 (INVITED).

41. "Use of Surface Behavior Diagrams to Determine Hydration Inhibitor Properties for Improved Durability of Aluminum Adhesive Bonds" G.D. Davis, J.S. Ahearn, and J.D. Venables, AIME Annual Meeting, New York, 26 February 1985.

42. "Environmental Durability of Phosphoric-Acid-Anodized Aluminum Adhesive Joints Protected with Hydration Inhibitors," J.S. Ahearn and G.D. Davis, Adhesion Society Meeting, Savannah, GA, 26 February 1985.

43. "The Applications of Surface Behavior Diagrams to Adhesive Bonding," G.D. Davis, European Conf. on Applications of Surface and Interfacial Analysis, Veldhoven, The Netherlands, 14-18 October 1985 (INVITED).

List of Publications
Under ONR Contract N00014-80-C-0718

1. J.S. Ahearn, G.D. Davis, T.S. Sun, and J.D. Venables, "Correlation of Surface Chemistry and Mechanical Properties of Aluminum/Polymer Bonds," in Adhesion Aspects of Polymer Coatings, ed. K.L. Mittal (Plenum Press, New York, 1983), p. 281.

2. G.D. Davis and J.D. Venables, "Surface and Interfacial Analysis," in Durability of Structural Adhesives, ed. A.J. Kinloch (Applied Science, Essex, 1983), p. 43.

3. G.D. Davis, J.S. Ahearn, and J.D. Venables, "Hydration of Aluminum Adherends as Studied by Surface Behavior Diagrams," Proc. 15th Nat. SAMPE Tech. Conf. (Cincinnati, OH, 1983), p. 202.

4. J.D. Venables, "Adhesion and Durability of Metal/Polymer Bonds," in Adhesion 7, ed. K.W. Allen (Elsevier, NY, 1983).

5. D.A. Hardwick, J.S. Ahearn, and J.D. Venables, "Environmental Durability of Aluminum Adhesive Joints Protected with Hydration Inhibitors," J. Mater. Sci. 19, 233 (1984).

6. J.D. Venables "Adhesion and Durability of Metal/Polymer Bonds," J. Mater. Sci. 19, 2431 (1984).

7. G.D. Davis, J.S. Ahearn, and J.D. Venables, "Use of Surface Behavior Diagrams to Study Hydration/Corrosion of Aluminum and Steel Surfaces," J. Vac. Sci. Technol. A 2, 763 (1984).

8. G.D. Davis, J.S. Ahearn, and J.D. Venables, "Hydration Inhibitor Properties for Improved Durability of Aluminum Adhesive Bonds," Proc. Int. Adhesion Conf. 1984, (Nottingham, England, 1984), p. 12al.

9. G.D. Davis, J.S. Ahearn, L.J. Matienzo, and J.D. Venables, "Use of Hydration Inhibitors to Improve Bond Durability of Aluminum Adhesive Joints," J. Mater. Sci. (in press).

10 D.A. Hardwick, J.S. Ahearn, A. Desai, and J.D. Venables, "Environmental Durability of Phosphoric-Acid-Anodized Aluminum Adhesive Joints Protected with Hydration Inhibitors," accepted by J. Mater. Sci.

11. H.W. White, C.D. Crowder, nd G.P. Alldredge, "Study of Hydration Inhibitors on Aluminum Oxide Using Tunneling Spectroscopy and Molecular Electrostatic Potential Calculations," accepted by J. Electrochem. Soc.

12. C.D. Crowder, G.P Alldredge, and H.W. White, "Study of the Orientation of Thiourea Adsorbed on Aluminum Oxide by Tunneling Spectroscopy I: Molecular Electrostatic Potential Calculations for Thiourea and Urea," University of Missouri, Columbia, accepted by Phys. Rev B.

13. C.D. Crowder, H.W. White, and G.P. Alldredge, "Study of the Orientation of Thiourea Adsorbed on Aluminum Oxide by Tunneling Spectroscopy II: Comparison of Experimental and Calculated Intensities," University of Missouri, Columbia, accepted by Phys. Rev B.

Appendix I

Recommended Bonding Pretreatment Procedures

Three procedures for pretreating aluminum adherends (Table A-1) have been identified as appropriate for different situations. Each incorporates the NTMP treatment (for NTMP solution preparation. see Table A-2) which has been found to improve the durability of structures formed using FPL and PAA adherends. Although the first, the PAA process, provides the best bond performance, it requires a large power supply for anodization and consequently may be unsuitable for large structures. The FPL process involves only immersion and is feasible for larger components. Finally, the Pasa-Jell treatment is applied by brush and may be necessary for pretreatment of very large components or for repair of existing structures. Please note, however, that the Pasa-Jell treatment can be operator dependent since application is by hand and since the thioxtropic gel is harder to remove by rinsing. Although no data exist showing the NTMP treatment to be effective in improving durability of Pasa-Jell-treated bonded structures, the gel is similar to a thickened FPL solution and provides similar surface morphology and chemistry. It is expected, then, that NTMP would enhance the performance of adhesive bonds prepared by Pasa-Jell.

Table A-1

Aluminum Bonding Pretreatments

A. Phosphoric Acid Anodization

Process	Solution or Operation	Time (min)	Temperature (°F)
Solvent Clean	Chlorinated solvent (1,1,1-trichloroethane)		175 max
Alkaline Clean	Turco 4215 (special and additive)	10 – 15	150 ± 5
Rinse, immersion/spray	Clean tap water	2	65 –110
Rinse, immersion/spray	Clean tap water	5	100 –140
Water Breaks	Inspect for Water Breaks Do Not Dry		
Deoxidize	FPL sulfochromate etch	15	150
Rinse, immersion/spray	Deionized water[a]	2	65 –110
Water Breaks	Inspect for Water Breaks Do Not Dry		
Phosphoric Acid Anodize	Phosphoric acid 9-11 wt% in deionized water Apply DC voltage within 1 minute Raise voltage stepwise to 10 V DC+1	2 – 5	67-77
	Maintain 10 V DC+1 for Turn off current	20 – 25	
Rinse, immersion within 2 min	After current is turned off		
	Agitated and overflowing 300ppm NTMP solution[b]		10 – 15
Rinse, spray	Deionized water		
	Inspect Wet for Treatment Coverage and Water Breaks		
Oven dry	Clean dry air	30	175 max
Cool to room temperature	Clean air	120	Ambient
	Inspect for Presence of Anodic Coating		

---

a Fluorine contamination in the rinse water of the FPL process can be very detrimental to bond performance [J.M. Chen, T.S. Sun, J.D. Venables, and R. Hopping, SAMPE J. (July/August 1978) p. 22.]

b See Table A-11.

B. Forest Products Laboratory

Process	Solution or Operation	Time (min)	Temperature (°F)
Solvent Clean	Chlorinated solvent (1,1,1-trichloroethane)		175 max
Alkaline Clean	Turco 4215 (special and additive)	10 – 15	150 ± 5
Rinse, immersion/spray	Clean tap water	2	65 –110
Rinse, immersion/spray	Clean tap water	5	100 –140
Water Break	Inspect for Water Break Do Not Dry		
Deoxidize	FPL sulfochromate etch	15	150
Rinse, immersion/spray	Deionized water(a)	2	65 –110
Rinse, immersion	300 ppm NTMP solution(b)	15	
Rinse, immersion/spray	Deionized water	2	65 –110
Water Break	Inspect for Water Break		
Oven dry	Clean dry air	30	175 (80°C) max
Cool to room temperature	Clean air	120	Ambient
	Prime		

a Fluorine contamination in the rinse water of the FPL process can be very detrimental to bond performance [J.M. Chen, T.S. Sun, J.D. Venables, and R. Hopping, SAMPE J. (July/August 1978) p. 22.]

b See Table A-II

C. Pasa-Jell

Process	Solution or Operation	Time (min)	Temperature (°F)
Mechanically Clean	Sand with fine (250 or 320) aluminum oxide-coated abrasive		
Brush with polyethylene, polypropylene or fluorocarbon bristle brush	Pasa-Jell 105	15	100 max
Rinse, spray	Clean tap water	10	100 max
Rinse, spray	300 ppm NTMP solution[a]	15	65-100
Rinse, spray	Deionized water	2	65-100
Water Breaks	Inspect for Water Break		
Dry	Clean dry air		100 max
	Prime		

a See table A-II
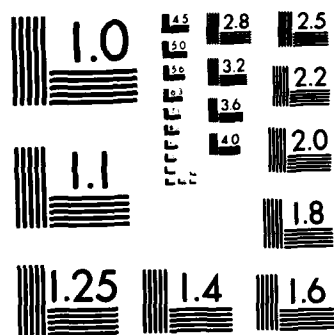
MICROCOPY RESOLUTION TEST CHART

NATIONAL BUREAU OF STANDARDS-1963-A

Table A-II

Preparation Procedure for 300 ppm NTMP Solution (4ℓ)

Add 2 ml 50wt% nitrilotris methylene phosphonic acid[a]
to 998 ml deionized, distilled water

Add 631 ml of this solution to 3369 ml deionized, distilled water.

[a] Aldrich Chemical Co., Milwaukee, WI

END

FILMED

6-85

DTIC